# Evaluation of On-chip Integration of Magneto-optic Isolators

by

Xiaoyan Chen

B.Eng. Electrical and Electronic Engineering
Nanyang Technological University, 2004

SUBMITTED TO THE DEPARTMENT OF MATERIALS SCIENCE AND ENGINEERING IN PARTIAL FULFILLMENT OF THE REQUIREMENTS FOR THE DEGREE OF

MASTER OF ENGINEERING IN MATERIALS SCIENCE AND ENGINEERING
AT THE
MASSACHUSETTS INSTITUTE OF TECHNOLOGY

SEPTEMBER 2007



Signature of Author _____
Department of Materials Science and Engineering
August, 2007

Certified by _____
Caroline A. Ross
Professor of Materials Science and Engineering
Thesis Supervisor

Accepted by _____
Samuel M. Allen
POSCO Professor of Physical Metallurgy
Chair, Department Committee for Graduate Students

**Evaluation of On Chip Integration of Magneto-optic Isolators**

**by**

**Xiaoyan Chen**

**Submitted to the Department of Materials Science and Engineering on August 10, 2007 in Partial Fulfillment of the Requirements for the Degree of Master of Engineering in Materials Science and Engineering**

# Abstract

The recent development of on chip integration of magneto-optic isolators is reviewed. Two major categories of structural designs for waveguide isolator (nonreciprocal mode conversion and nonreciprocal phase shift) have both merits and short comings for integration. The advances in integration techniques and materials related developments in the last decade are a big step towards monolithic integration of isolator with other optical devices. But whether or not the integrated magneto-optic isolators will penetrate the market eventually would also depend not its competing technologies.

Thesis Supervisor: Caroline A. Ross

Title: Professor of Materials Science and Engineering

# Acknowledgement

First I want to express my gratitude my advisor Prof. Caroline A. Ross for giving me this opportunity to work on the subject I am interested in. She has always been patient and supportive in all the matters whenever I presented to her. I also want to thank Prof. Wong Chee Cheong in NTU and Dr. Tang Jinghua in IMRE for their helpful comments and fruitful discussions we had.

My time in MIT was short, but I had such wonderful experience that is almost impossible to get anywhere else. The passions and enthusiasm from professors and dedicated classmates are always motivational and inspirational. I would like to thank all of those who helped and supported me to get here, especially to Judy Zou and Lirong Zeng, from whom I have learnt a great deal. I am so happy that we become close friends in such a short time. Special thanks go to my friend Anindya Benerjee for his advice, help, support and many enjoyable conversations we had in the past year.

For *alma mater*, my thanks go to Prof. Perry Shum for introducing me to wonders of research and constant encouragement, which has been instrumental for me to reach what I am now.

I cannot thank my parents enough for their love and being always supportive for my endeavor. I will always do my best to make them proud.

# Table of Content

# 1. Introduction

Optical communication via glass fiber is an attractive technique for high data rate and long distance transmission. Semiconductor lasers are available as reliable light sources. It is essential that the laser are protected from reflected light, otherwise they can become unstable or can even be damaged. For this purpose optical isolators which rely on the nonreciprocal Faraday rotation of magneto-optical materials, are needed.

The rapid development of optical fiber communication systems requires a high level of on-chip integration of various optical components. Optical integration doesn't have the same degree of success as electronics integration. Since 1958, from the first integrated circuit (IC) to today's high-end microprocessors that contain over millions of transistors on a single chip, the vast development in IC attributes to the advanced technology in silicon fabrication. For both systems, there are two primary benefits or the main motivations for integration: increasing performance and significantly lower costs. Unlike electronic integration, optical integration involves assembling components that either perform different functions or are made from different materials. The method of integration is critical for the gains in performance and cost. So the application and market size determine which device should be integrated.

As mentioned earlier, the isolator an indispensable part of laser system, thus we won't achieve complete integration or even subsystem integration without integrating the it. However, today's conventional optical isolators utilizing non-planar geometries are bulky and require expensive alignment technique. There is a need in the industry for inexpensive isolators that can be integrated with other optoelectronic devices on a single chip. Different ideas have been explored over the last 20 years to solve this problem, ranging from the conventional to the unconventional ones. In this work, I present a discussion of the developments in this field over the last decades and some of the important issues in the design and fabrication of optical waveguide isolators. Theoretical derivation and experimental details will be presented whenever necessary to facilitate understanding; however they are not the main focus of the thesis.

In order to appreciate the challenges to the on-chip optical isolators, the first section will consider the standard operational principle in bulk devices and the typical materials used. The various structural designs for waveguide isolator based on garnet materials are then presented. Integration techniques and materials issues associated with monolithic integration are evaluated in a separate section, where both conventional garnets and novel non-garnets materials and various material growth techniques are reviewed. Finally, a competitive and market analysis is presented in the last section, where competing technologies and market demand are discussed.

# 2. Conventional Bulk Optical Isolators

## 2.1 Faraday Rotation

More than 150 years ago, Michael Faraday discovered that linearly polarized light traveling through a substance experiences a rotation when a magnetic field is applied to the material. The amount of rotation $\varphi$ was found to be proportional to the magnitude of the magnetic field H and to the length of the sample L, $\phi = VHL$, where the constant of proportionality $V$ is called the Verdet constant.

A linearly polarized beam of light with a unique electric field can be decomposed into two circularly polarized beams of equal intensity. These right- and left-circularly polarized beams propagate simultaneously, but are independent of each other (orthogonal). For instance, the field E, which is traveling at a certain phase velocity can really be thought of as a superposition of field $E_+$ and $E_-$ traveling at $c/n_+$ and $c/n_-$, respectively [1]. Therefore, the plane of polarization of the light will rotate through an angle $\phi = \frac{\omega L}{2c}(n_+ - n_-)$. An applied magnetic field causes the material to become optically active – producing different refractive indices for the two beams so that they travel at different phase velocities. The physical origin of these different indices of refraction can be thought of as magnetic-field-induced Larmor precession of electron orbits. Therefore, $n$ now becomes a function of ω, such that $n_+ - n_- = \frac{dn}{d\omega}\frac{e}{mc}H$. Thus, after passing through the material, the two beams have a different phase relationship, resulting in a rotation of the E-vector of the combined beams. The propagation of the beam of light has to be parallel to the direction of the magnet field in order to observe the rotation in its plane of polarization. If the field is perpendicular to the beam, then there is no rotation. And also there should be a medium present where the beam and the magnetic fields will interact [2]. When non-magnetic materials like copper, lead, tin and silver are placed between the magnets, they cause no effect to polarized waves [3].

It is important to note that the sign of $\phi$ does not depend on the sign of the wavevector of the incoming wave, but only on the sign of $H$, which is known as nonreciprocality. It means when a wave propagates through the medium and then is reflected back along the same path will undergo a rotation of $\phi$ during the first trip and another $\phi$ rotation during the trip back. So the total rotation with respect to the original polarization is $2\phi$ instead of 0. This principle is absolutely essential to the construction of optical isolators.

## 2.2 Bulk Optical Isolators

### 2.2.1 Polarization-Dependent Type

In bulk devices, optical isolators are common and their design is fairly well understood. Commercial optical isolators generally consist of (1) a magnetic garnet crystal having a faraday effect, (2) a permanent magnet for applying a designated magnetic field, and (3) polarizing elements with polarization axes offset of 45°. A schematic of the structure is presented in Figure 2.1. A forward light passing the optical isolator undergoes the following: (1) after passing through the polarizer, the incident light is transformed into a linearly polarized light; (2) after passing through the Faraday rotator, the polarization plane is rotated 45°; (3) this light passes through the analyzer without loss since its polarization plane is now in the same direction as the light transmission axis of the analyzer. In contrast, a backward light undergoes a slightly different process: (1) after passing through the analyzer, the backward light is transformed in to a linearly polarized light with a 45° tilt in the transmission axis; (2) after passing through the Faraday rotator, the polarization place of the backward light is rotated 45° in the same direction as the first trip; (3) this light is completely shut out by the polarizer because its polarization plane is now 90° away from the light transmission axis of the polarizer. The performance of optical isolators is primarily evaluated by their insertion losses and isolation ratio (the ratio of the optical power propagating backward at the input to the forward power at the output), both of which are determined by the absorption losses end-face reflectance and the extinction ratios of optical elements. Commercially available isolators can achieve isolation ratio of -30 to -65 dB [4].

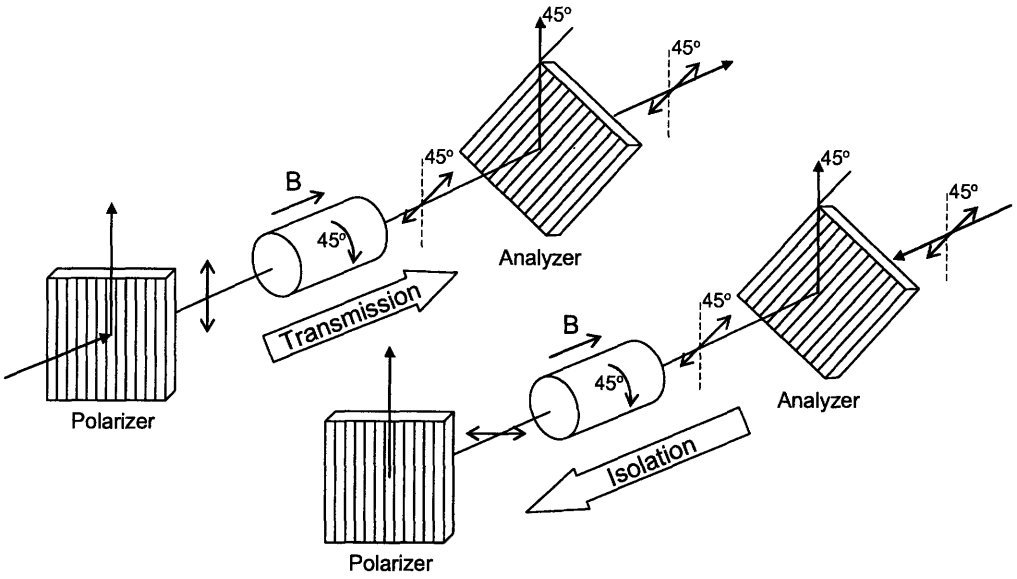


Figure 2.1 An optical isolator transmits light in one direction (a) and blocks light in the opposite direction (b).

### 2.2.2. Polarization-Independent Type

While polarization-dependent optical isolators transmit only the light polarized in a specific direction, polarization-independent isolators transmit all polarized light. Consequently, these isolators are frequently used in optical fiber amplifiers. The basic working principle of a polarization-independent optical isolator was first proposed by Matsumoto [5]. Its arrangement consists of a Faraday rotator and half-wave plate inserted between a pair of birefringent crystal plates of equal thickness (as spatial work-off polarizer, SWP). The birefringent plate functions to split the incident beam into a pair of orthogonal rays and separate one ray ("E" ray) from the other ray ("O" ray) as they travel through the plate. This phenomenon of spatial displacement is often referred to as "walk-off". The two separated components are rotated as they pass through the half wave plate and Faraday rotator and then enter the second birefringent plate where they are recombined to form the output signal. Since a Faraday rotator is a nonreciprocal device, any signal traveling in the reverse direction through the isolator will be physically separated into orthogonally polarized signals as it passes through both birefringent plates and will not recombine into the input fiber. In an alternative design, a wedge-shaped

spatial walk-off polarizer was used to bring a large separation of the two polarization states in backward direction by Shirasaki [6]. The schematic and working principle is depicted in Figure 2.2.

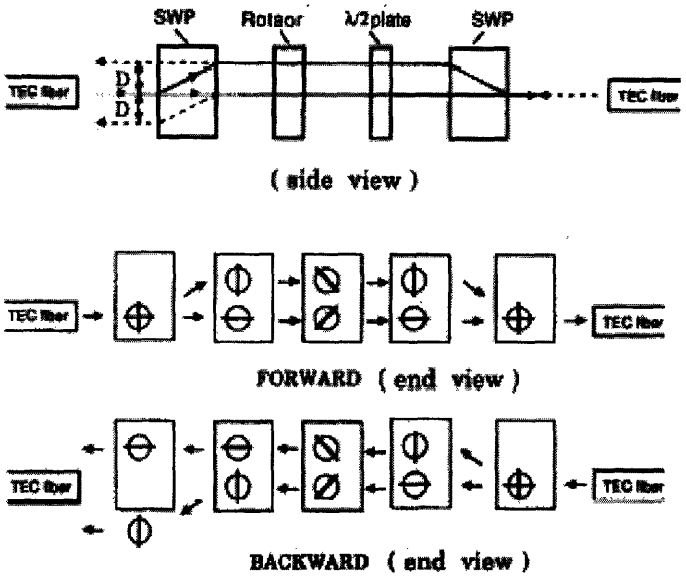


Figure 2.2 Schematic diagram of fiber-embedded polarization-independent isolator and its principle of operation. The above figure and caption are from [6].

## 2.3 Magnetic Garnet Crystal

Garnet crystals are the typical materials used in bulk isolators to achieve high Faraday rotation coefficient with low optical losses. The chemical formula of garnets is $\{c^{+3}\}[a^{+3}](d^{+3})O_{12}$ [7]. That means, there are three different lattice sites for the cations with respect to the surrounding oxygen anions. The conventional unit cell of a garnet, shown in Figure 2.3, contains 164 ions. The dodecahedral sites {c} are occupied by rare earth cations and the octahedral [a] and tetrahedral (d) sites are for iron. The [a] and (d) sublattices are coupled antiferromagnetically, which yields a ferromagnetic crystal due to the nonequivalent sublattices. The saturation magnetization $M_s$ given in Dötsch's work is the vectorial sum of sublattice magnetizations: $M_s(T) = M_d(T) - M_a(T)$, where $M_d$ and $M_a$ denote the saturation magnetization of the tetrahedral and octahedral sublattices, respectively [7]. The Faraday rotation of the garnets depends on temperature T, the optical wavelength λ and the sublattice magnetizations.

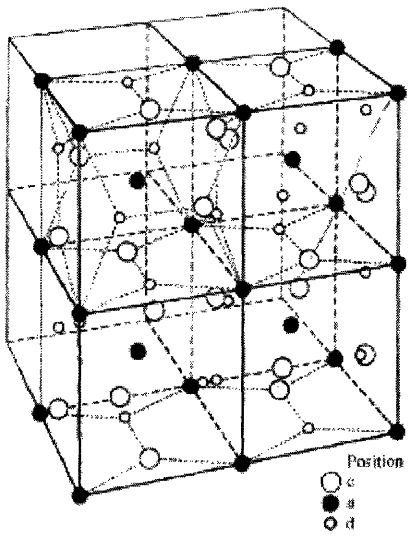


Figure 2.3 Arrangement of cations in the garnet structure from *Physics of Magnetic Garnets*, A. Paoletti (ed.), New York: North-Holland, 1978.

The most commonly used materials include the ferromagnetic garnet yttrium iron garnet, $Y_3Fe_5O_{12}$ (YIG) and Gallium Gadolinium Garnet, $Gd_3Ga_5O_{12}$ (GGG), and variations including Bi-YIG (bismuth-substituted yttrium iron garnet), which can strongly enhance the Faraday rotation. An even much higher Faraday rotation is possible, if cerium is substituted into the garnet crystals instead of bismuth [9]. Although cerium causes increased optical losses, the figure of merit, Faraday rotation per damping is still better than for the bismuth substituted films. Other nonreciprocal materials include terbium gallium garnet, $Tb_3Ga_5O_{12}$ (TGG), berbium aluminum garnet, $Tb_3Al_5O_{12}$ (TbAlG) and terbium doped borosilicate glass TbGlass. TGG is used for wavelengths between 500 and 1100nm, and YIG is commonly utilized between 1100 and 2100 nm [9]. Magnetic garnets can be grown as bulk crystals and also film on garnets substrate can be obtained by epitaxial method, such as liquid phase epitaxy (LPE) [10], sputter epitaxy (SE) [11] and pulsed laser deposition (PLD) [12].

# 3. Structures of Waveguide Optical Isolators

Faraday rotation is the standard method of obtaining non-reciprocity in bulk optical elements. However, it is not so straightforward to reproduce it in an integrated format. There are many challenges in adapting these approaches to optoelectronic integrated circuit (OEIC). First, the planer structure breaks the symmetry of bulk devices, called shape birefringence. Moreover, as film-based devices, different films will be deposited on a substrate, which lead to second type of birefringence: lattice mismatch. These effects are undesirable as they disrupt the conversion efficiency between the modes, which yields elliptically polarized light. In optical isolators, this severely degrades the isolation since elliptically polarized light is not completely blocked by the polarizer. There are different attempts to overcome these effects over the years, with different degree of success regard to isolation efficiency and insertion loss. Second, when integrating magneto-optic components with semiconductor materials, further difficulties arise, e.g. difference in refractive index and growth method incompatibility. Third, for an isolator based on Faraday rotation there must be magnetic field provider and polarization selectivity. This section focuses on the various structural designs of standalone waveguide isolators, whereas integration and materials issues will be addressed in the following section.

## 3.1 Theoretical Background

Some basic theory behind the waveguide magneto-optics is summarized in this section, based mainly on the work by Dötsch, *et al.* [7]. A simple rib waveguide typically used in integrated optics is shown in Figure 3.1. It is assumed that the waveguides are prepared in an isotropic, dielectric material and is homogeneous in z-direction, the direction of light propagation. Different numerical methods can be used to model the field profiles, such as finite element (FEM), finite difference (FDM), film mode matching (FMM), beam propagation (BPM), or wave matching method, which is based on a transverse resonance technique [14].

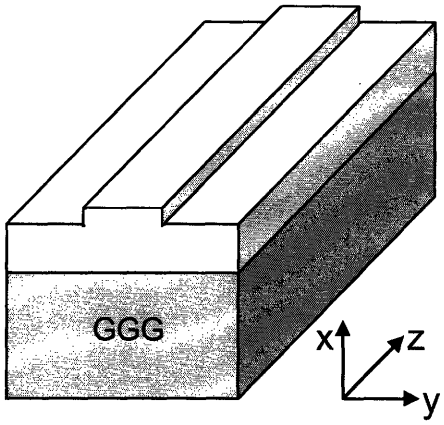


Figure 3.1 Simple rib waveguide with magneto-optic material core on GGG substrate.

### 3.1.1 Magneto-optical Effects

The Magneto-optic properties are introduced by perturbation theory. We assume the substrate and cover layers to be made of lossless isotropic material with homogeneous permittivity $\varepsilon_s = n_s^2$ and $\varepsilon_c = n_c^2$. The permittivity tensor for the Magneto-optic core region is split into the contribution of an isotropic lossless refractive index $n_f$ and a residual $\Delta\varepsilon$, a perturbation as [7]:

$$\varepsilon_f = n_f^2 \begin{bmatrix} 1 & 0 & 0 \\ 0 & 1 & 0 \\ 0 & 0 & 1 \end{bmatrix} + \Delta\varepsilon = n_f^2 \begin{bmatrix} 1 & 0 & 0 \\ 0 & 1 & 0 \\ 0 & 0 & 1 \end{bmatrix} + K \begin{bmatrix} 0 & M_z & -M_y \\ -M_z & 0 & M_x \\ M_y & -M_x & 0 \end{bmatrix} \qquad 3.1$$

$M_j$, $j$= x, y, z denotes the direction of the magnetization. K is a complex material parameter $K=K'+iK''$, where K' determines the Faraday ellipticity. The core permittivity contribution due to the linear Magneto-optic effect can be written

$$\Delta\varepsilon_{mo} = iK'' \begin{bmatrix} 0 & M_z & -M_y \\ -M_z & 0 & M_x \\ M_y & -M_x & 0 \end{bmatrix} \qquad 3.2$$

and K'' relates to Faraday rotation by

$$\Theta_{F,sat} = -k_o \frac{K'' M_s}{2n_f} \tag{3.3}$$

### 3.1.2 Nonreciprocal TE-TM Mode Conversion

When the magnetization component is in z direction, $M_z$, which is parallel to the waveguide axis, the tensor $\Delta\varepsilon$ couples the x-component of the quasi TE mode to the y-component quasi TM mode and it leads to periodical power exchange between these modes and thus yields mode conversion. This is similar to Faraday rotation in bulk media. Hence the optical isolators built based on mode conversion are usually categorized by the adaptation of Faraday rotation scheme in waveguide isolation [4].

By perturbation theory, Dötsch [7] denotes the z-dependent amplitudes of the normalized modes by $A^{TE}(z)$ and $A^{TM}(z)$, which are varying along z-direction. Assuming that the propagation starts with a purely TE polarization wave, after propagating along the device of length L, by mode conversion, the power of TM polarized mode to TE polarized mode is

$$\frac{\left|A^{TM}(L)\right|^2}{\left|A^{TE}(L)\right|^2} = \frac{|k|^2}{|k|^2 + \frac{\Delta\beta^2}{4}} \sin^2\left(L\sqrt{|k|^2 + \frac{\Delta\beta^2}{4}}\right) \tag{3.4}$$

where $k$ is the coupling constant $k = \frac{\varpi\varepsilon_0}{4}\int\int \vec{E}^{*TE}\Delta\varepsilon\vec{E}^{TM}\,dxdy$ and $\Delta\beta = \beta^{TM} - \beta^{TE}$.

From Eqn. 3.4 we can see that a complete mode conversion needs a perfect phase matching $\beta^{TM} = \beta^{TE}$.

### 3.1.3 Nonreciprocal Phase Shift

The transverse magnetization components $M_x$ and $M_y$ can induce a change in the propagation constant $\beta$, which also depends on the propagation direction, +z or –z:

$$\beta^{+z} = \beta + \delta\beta \text{ and } \beta^{-z} = \beta - \delta\beta. \tag{3.5}$$

Hence, the resulting difference between the forward and backward propagation constant is $\Delta\beta = 2\delta\beta$ . "This nonreciprocal phase shift doesn't exist in the case of light propagation in bulk materials, because the effect can be viewed as being immediately related to material discontinuities. A simple plausible explanation can be given using the rough zigzag model of mode propagation in dielectric waveguides. Each reflection at the waveguide boundaries induces a phase shift which depends on the polarization, TE or TM." [7]. If magnetization is in x-direction, which is along the normal of the substrate, a nonreciprocal phase shift for the TE mode will be

$$\Delta\beta^{TE} = \frac{2\omega\varepsilon_0}{\beta^{TE} N}\int\int(K'' M_x)E_y \partial_y E_y dxdy \tag{3.6}$$

normalized by the power flow in z-direction $N$. And for TM mode, the nonreciprocal phase shift is induced by y-direction magnetization $M_y$ which is in plane with the substrate surface and transverse to light propagation direction,

$$\Delta\beta^{TM} = \frac{2\beta^{TM}}{N\omega\varepsilon_0}\int\int\left(\frac{K'' M_y}{n_f^{\,4}}\right)H_y \partial_x H_y dxdy \tag{3.7}$$

The double integral can be treated as single integrals along the boundaries where discontinuity occur if it is assumed that the waveguide cross section can be divided into rectangles where the material parameters are constant. To achieve a large nonreciprocal phase shift, it is essential to have a strong discontinuity of Faraday rotation. The magnitude and sign of the nonreciprocal phase shifts depend on the magnitude and sign of the Faraday rotation and the geometry of the waveguide [7].

## 3.2 Nonreciprocal Mode Conversion Faraday Rotators

This fundamental concept for integrated isolators has been first treated by Yamanoto and co-workders [15]. If the magnetization is parallel to the propagation direction, Faraday rotation causes coupling between TE and TM modes. The major issue of this concept is the phase mismatch between TE and TM modes due to the problems inherited with the waveguides. The main difficulties come from the complexity of fabrication and

stringency of the tolerances required for phase matching [4]. Nevertheless, constant efforts are put in by a number of researchers over the years. We will see the different designs that have been proposed and realized in this section.

### 3.2.1 Birefringence in Garnet Film Waveguide

Undoubtedly the material system which has seen the greatest research activity in magneto-optic waveguide devices is garnet. These systems usually consist of thin-film ion garnets (e.g. yttrium iron garnet YIG) grown on a gadolinium gallium garnet (GGG) substrate. Epitaxial films can be grown with excellent optical quality, large Faraday rotation and low optical absorption in the hear-infrared region. The garnet thin film waveguide isolators have potential advantages over the competing bulk crystal garnets which are currently used in magneto-optic devices, including their low magnetic field requirement for in-plane magnetic saturation, and the elimination of lens when corporate with the rest of optical system.

The developments of this kind of isolator focus mainly on the reduction or elimination of birefringence in the thin film waveguide. Three mechanisms giving rise to linear birefringence have been identified in the waveguide formation process: shape or geometrical birefringence, stress-induced or photoelastic birefringence, and growth-induced birefringence. A fourth effect is magnetic linear birefringence, which is observed when the magnetization is perpendicular to the direction of propagation of the light. This effect will be neglected here since the nonreciprocal mode conversation always requires parallel magnetization to the light propagation direction. Various methods have been developed to reduce these effects either individually or zeroing out the net birefringence.

- *Shape birefringence* is the difference between the propagation constants of the TE and TM modes that propagates in a film. The refractive indices of the TE modes are larger than those of the corresponding TM modes. Shape birefringence increases with the optical wavelength and decrease the thickness of the film.

A symmetric cross section in the waveguide can, in principle, reduce the shape-induced birefringence [4]. LPE-grown buried-channel substituted-YIG waveguides have been realized through wet etching techniques, followed by cladding overgrowth, shown in Figure 3.2 [16]. A triangular cross-section waveguides is formed by crystallographic etching with isolation ratios of -20dB at 1.3 μm. By comparing $\Delta\beta$ of $30^{\circ}$/cm ($\Delta\beta = \beta^{TM} - \beta^{TE}$) for the etched channel waveguide with $\Delta\beta$ of $1070^{\circ}$/cm of the not etched region of the same wafer, there is a significant reduction but not complete elimination of shape birefringence.

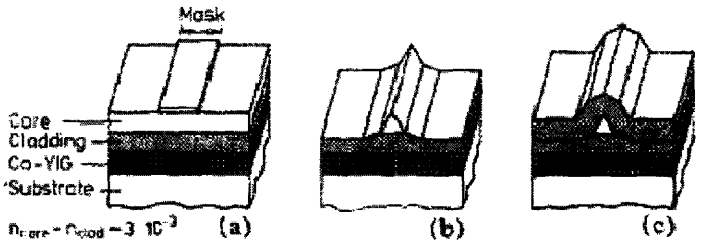


Figure 3.2 Fabrication of buried channel waveguides in YIG: (a) planar single-mode waveguides. The typical thickness of each individual layer is about 5 μm; (b) etched rib waveguide; (c) buried channel waveguide [16].

Sugimoto *et al.* reported higher extinction ratio (up to -31dB at $\lambda$ = 1.5 μm) [17]. A buried square channel waveguide was obtained through the anisotropic dry etching followed by wet-etch smoothing, with schematic shown in Figure 3.3.

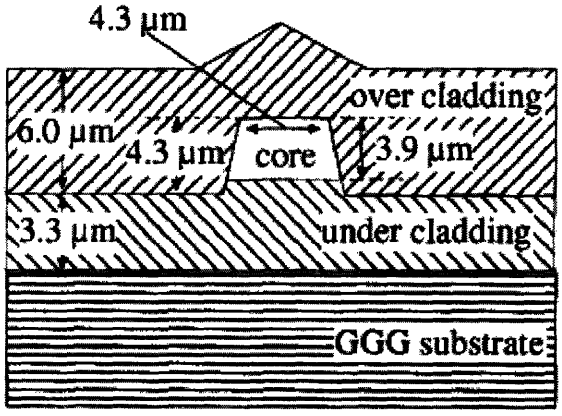


Figure 3.3 Schematic sketch of a cross section of a typical buried channel waveguide [17].

Multilayer films have the effect of reducing birefringence of this kind also. Single-mode films can be made by growing double or triple garnet films on GGG [18, 19]. An intermediate layer grown in between of the active magneto-optic film and the GGG substrate could reduce the birefringence and increase the conversion efficiency. The mode conversion in a four-layer (air-cladding-intermediate-substrate) waveguide has been demonstrated [18]. According to mode coupling theory, the TE-TM mode conversion efficiency F is given by

$$F = \left[1 + (\Delta\beta / 2\theta_F)^2\right]^{-1} \tag{3.8}$$

where $\Delta\beta$ ($m^{-1}$) is the propagation constant difference between TE and TM mode, and $\theta_F$ ($m^{-1}$) is the specific Faraday rotation. The Faraday rotation $\theta_F$ depends on the guide layer materials and the propagation constant difference $\Delta\beta$ depends on waveguide structure. In the four-layer waveguide, a small difference $\Delta n$ in refractive index between guiding layer ($n_1$) and intermediate layer ($n_2$) can result in a high conversion efficiency as illustrated in Figure 3.4 [18].

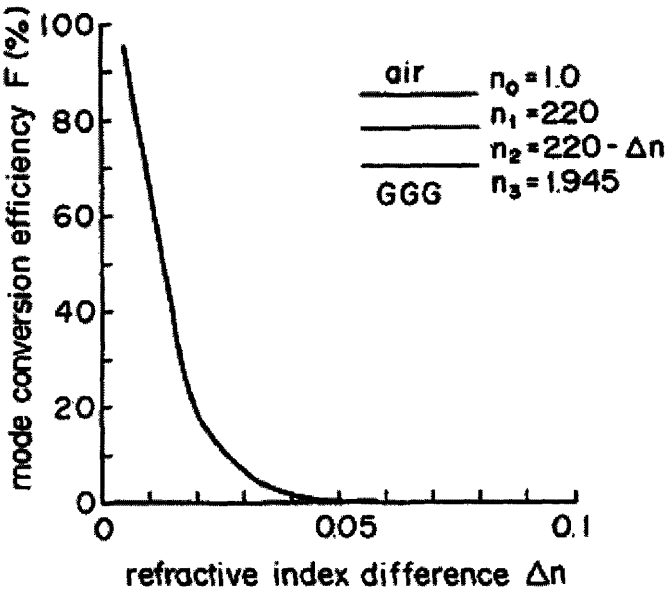


Figure 3.4 Relation between TE-TM mode conversion efficiency $F$ and refractive-index difference $\Delta n$. [18]

At $\Delta n$ =0.005, $F$ = 94.6% is possible, but the refractive-index control of both guide and intermediate layers becomes difficult. A solution that yields both high mode conversion and the proper value of $\Delta n$ is given by using an appropriate film overcoated on the guide layer instead of air as the cladding layer. By properly choosing the cladding layer, a maximum 98.2% mode conversion efficiency F can be obtained.

- *Stress-induced birefringence* is observed in any epitaxial film which has a lattice constant different from that of its substrate.

Even when the asymmetries have been reduced, the internal stress due to mismatch strain remains in the crystal as a source of linear birefringence. Dammann, *et al.* [20] introduced a method to tune the stress-induced birefringence by applying external stress to the waveguide. In the experiments, a pneumatic table has been used to generate external pressure, and piezoelectric elements can be employed in working isolators. Experiments demonstrated that by applying an external stress between 0 to 1.6 kN/cm$^2$, a tuning range for $\Delta\beta$ of 250$^\circ$/cm was achieved. Though the results showed that stress-induced birefringence can be reduced by external means, no working isolator was produced.

- *Growth-induced birefringence* is found during the film growth process. When more than one type of atoms occupies the dodecahedral Y site in garnet crystals, the nonrandom distribution associated with directional growth from the flux, gives rise to growth induced magnetic and optical anisotropy. The magnitude and sign can vary depending on the garnet composition, crystal orientation and growth conditions. And it is independent of film thickness or wavelength [21].

High temperature annealing was found to have great effect in reducing growth-induced birefringence in liquid-phase-epitaxial-grown (LPE) Bi-substituted iron garnet films [22]. The garnet crystal has three different crystallographic sites as described in section 2.3., i.e. dodecahedral, octahedral, and tetrahedral sites. Bismuth and lanthanoid ions occupy the dodecahedral sites. Iron and gallium ions distributed over both of the octahedral and tetrahedral sites. A deformation of the microscopic structure around

bismuth ions seems to be responsible for the anisotropy. It can be minimized by growth at the highest possible temperature or high temperature annealing.

- *Total linear birefringence* (shape, stress and growth-induced birefringence) can be reduced by zeroing out the net effects, utilizing one source of birefringence against another one.

Wolfe *et al.* suggested that control of the shape birefringence after film growth maybe the best way to achieve zero birefringence by canceling it with stress induced part [21,23]. The refractive indices of the TE modes are larger than those of the corresponding TM modes in shape birefringence, so it is defined as positive ($\Delta\beta = \beta^{TE} - \beta^{TM} > 0$). In stress-induced term, the lattice constant of the Bi-YIG films are larger than that of the GGG substrate, and the films are in compression. In this case, the refractive index for the $TM_0$ mode is larger than that for the $TE_0$ mode. Therefore, the stress birefringence and the shape birefringence are opposite in sign and comparable in magnitude with strains of the order of $10^{-4}$. Furthermore, the shape birefringence has a strong inverse relationship with film thickness while stress birefringence is independent of it. After the film is annealed to reduce the growth-induced birefringence to zero, the remaining linear birefringence can then be reduced to zero by either thinning the top active film using chemical and plasma etching or increasing its thickness by depositing a covering dielectric layer. The effect of etching is schematically shown in Figure 3.5 [24]. For the case illustrated in the figure, the top film is grown in compression and has been annealed to achieve zero growth-induced birefringence. Its thickness is such that the positive shape birefringence is smaller than the negative stress birefringence, hence reducing its thickness will give zero total birefringence.

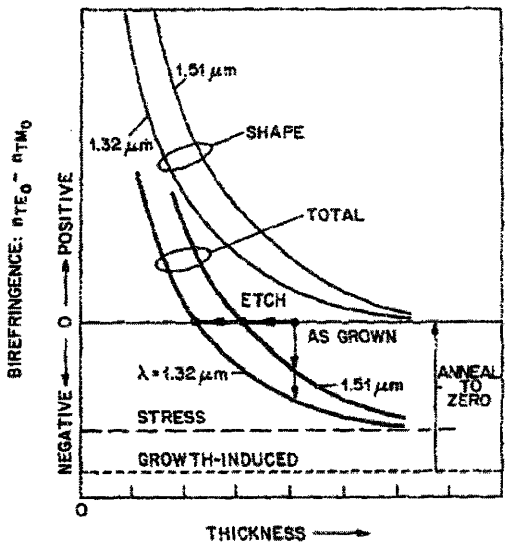


Figure 3.5 Shape, stress, and growth-induced linear birefringence vs thickness in a magneto-optic waveguide (schematic). [24]

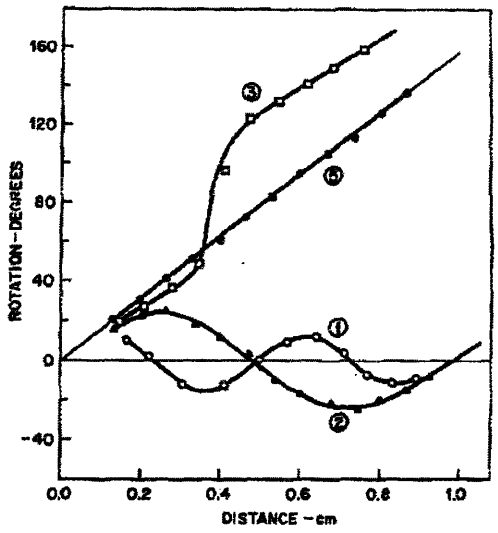


Figure 3.6 Faraday rotation vs. distance in a double Bi-YIG film after wet etching for (1) 0 min, (2) 10 min, (3) 18 min and (5) 24 min. [24]

Experimental demonstration of the effect of film thinning is shown in the form of rotation angle versus distance in Figure 3.6 [24]. The as grown film had a birefringence period of 0.48cm at wavelength of 1.32 μm. As the film thickness was etched thinner, the total linear birefringence decreased and the period of oscillation increased. With further

thinning, the rotation increased monotonically with distance. Curve 5 with an etching time of 24 min and film thickness of 2 μm in Figure 3.6 is where the shape birefringence just cancels the stress effect, the total linear birefringence is zero and only the Faraday rotation remains. However, if the negative compressive stress is too large, it may be necessary to thin the film so much that this layer no longer supports any modes. For such etch-tuned waveguide devices, this technique is advantages only in thick-film devices. This process is tedious and only makes sense for research curiosity. For production, more manufacturing-compatible process needs to be developed.

### 3.2.2 Quasi-phase Matched Faraday Rotator

Phase mismatch between the birefringence of the films normally results in an oscillatory behavior in Faraday rotation between small positive and negative angles [25]. Quasi-phase matching (QPM) of these birefringences through a periodic reversal of the sign of the Faraday coefficient along the waveguide direction can overcome these problems. This was first demonstrated by Tien *et al.* [26] that they used a serpentine electrical circuit with a period equal to one-half of the birefringent period (the propagation distance over which the state of polarization repeats itself). The Faraday reversal can also be built into the garnet film by a permanent reversal of the sublattice magnetization, which was produced by localized laser annealing of garnet films with a specially designed composition [25]. The experiment was performed on bismuth and gallium substituted YIG on GGG substrate. Multimode cw argon ion laser with a power 10% below the threshold for crystal damage was used to reverse the sublattice dominance and thus the sign of the magneto-optical rotation at one half of the birefringent period. Figure 3.7 shows the polarization rotation angle as a function of distance. The curve of unannealed film with oscillating behavior was used to determine the birefringent period. In the film with laser annealed bands, the rotation increased monotonically with distance.

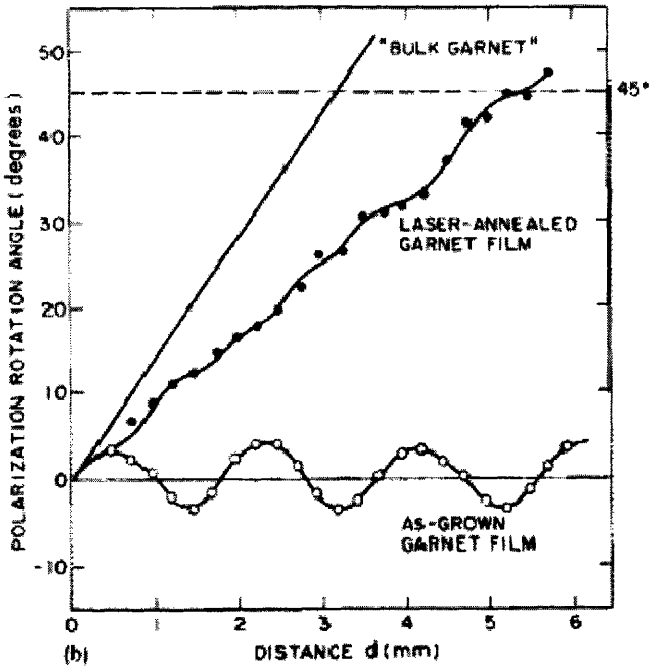


Figure 3.7 Polarization rotation for 1.45 μm light vs propagation distance in a 2.8 μm LPE film of (Bi, Ga) YIG on a GGG substrate. The "bulk garnet" line was calculated for a material with the same Faraday coefficient (140°/cm) and no birefringence [25].

Holmes *et al.* [27] defined the characteristic beat length of the oscillatory behavior of the polarization as

$$L_{\Delta\beta} = \frac{\pi}{\sqrt{(\Delta\beta_{brf})^2+(\Delta\beta_{MO})^2}} \approx \frac{\pi}{\Delta\beta_{brf}}, \qquad 3.9$$

where Magneto-optic (MO) birefringence $\Delta\beta_{MO}$, the sum of sublattice contributions when introducing MO elements into waveguide structures is a lot smaller compared to $\Delta\beta_{brf}$. They extended the nonlinearity in optics to Faraday rotation by utilizing an upper cladding that periodically alternates between MO and non-MO media (Figure 3.8). This approach realizes the continuous III-V waveguide core propagation. It requires monodirectional magnetic field, and avoids the complications arising from magnetic field edge effects and potential demagnetization at the interfaces between the alternately magnetized elements [27]. The quasi-phase matching concept in cladding layer could achieve the similar effect as that in core layer (Figure 3.8b). It has not been possible to

obtain a quantitative value for actual conversion efficiency, but they predicted 60 times higher than the case in the absence of phase-matching.

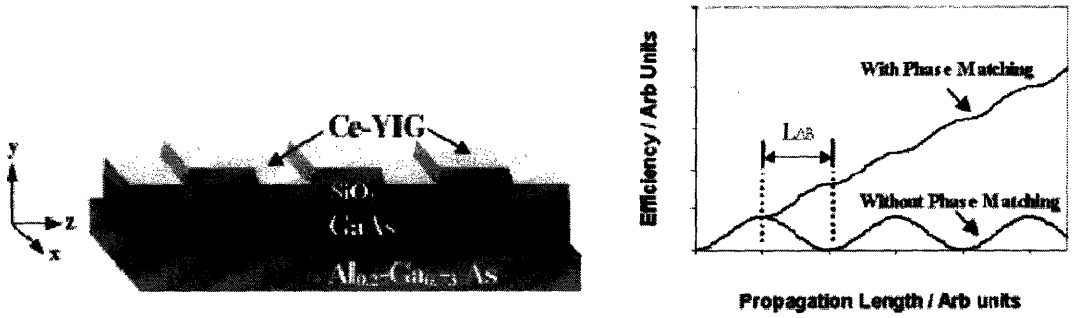


Figure 3.8 (a) Schematic of QPM waveguide structure. It consists of a 4.7 μm $Al_{0.27}Ga_{0.73}As$ lower cladding and a 0.5 μm GaAs core layer. A 200 nm $SiO_2$ is deposited and patterned with 50% duty cycle period and Ce-YIG is sputtered. (b) Schematic demonstrating QPM by periodic domain reversal. [27].

### 3.2.3 Input Polarization Angle Approach for Rotator with phase mismatch

Since it is extremely difficult to reduce the linear birefringence to zero in practice, Dammann *et al* .[28] showed that a perfect extinction of backward propagating light can be achieved if the input polarization angle is properly chosen in a magneto-optic waveguide with nonzero linear birefringence. This "trick" is simply to rotate the input and output polarizers by 22.5° from the principal waveguide direction. It was demonstrated theoretically by visualizing the mode coupling as "coupling tracks" on the Poincaré sphere representation for the states of polarization.

Wolfe *et al.* extended this method suggested by Dammann to etch-tuned ridge waveguide isolator and isolation ratios between -32 and -37 dB have been measured over a wavelength range from 1.43 to 1.58 μm and over a temperature range of ± 30 °C [29]. In a pure etch-tuned ridge waveguide isolator [21], the linear birefringence is tuned to zero at one chosen wavelength only. For light entering the waveguide in the TE or the TM mode, isolation is perfect only at this one wavelength. Using the Dammann's "trick", perfect isolation can be achieved over a wide range of wavelengths since no strict phase match is required. The main limitation of this method is the induced excess loss in the

forward direction for which elliptically polarized light is obtained at the end face of the waveguide. The excess forward loss obtained by Wolfe et al. was 1dB or less over the wavelength range of ± 0.2 μm. This method provides the one possibility to solve the $\Delta\beta$ problem without the need of phase matching $\Delta\beta \rightarrow 0$.

## 3.3 Nonreciprocal Mach-Zehnder Interferometer Based Isolators

The enormous difficulties to achieve precise phase matching induced the investigation of other isolator concept. A new concept of isolator based on nonreciprocal phase shift using Mach-Zehnder configuration was first proposed by Auracher and Witte as far back as 1975 [30]. The application of a transverse magnetic field to the propagation direction induces the coupling of longitudinal and transverse components of the optical field, resulting in different propagation constants for forward and backward directions $\Delta\beta = \beta_{forw}^{TM} - \beta_{back}^{TM}$ . This induces a nonreciprocal phase shift of the propagating mode. Different isolation schemes have been proposed and implemented. Most of them reply on constructive interference in forward direction and destructive interference in the backward direction [30-45]. For example, with proper arm length designed in Mach-Zehnder interferometer, in forward direction, waves propagating along both arms of the Mach-Zehnder interferometer are in phase, while in backward direction a phase shift of $\pi$ occurs to form destructive interference. This type of device operates within a distinct mode and does not require tight control of birefringence. Also no polarizers are needed since it relies on the destructive interference of backward propagating waves.

### 3.3.1 TM Mode Nonreciprocal Phase Shift Isolators

The first illustration of isolator of this type was TM mode [30]. It was not until 1998 that the TE mode nonreciprocal phase shift isolator was investigated. Figure 3.9 shows the working principle of Mach-Zehnder interferometer (MZI) waveguide isolator for transverse magnetic (TM) mode. The Y coupler (A) splits the input light into two beams of equal amplitude and in phase. Nonreciprocal elements are incorporated in both arms of the interferometer and they provide a positive or negative 90° phase shift between the two arms depending on the propagating direction. The magnetizations are at opposite

direction as indicated in the figure in order to achieve such phase shift. For the interferometer to work as an ideal isolator a positive 90° reciprocal phase shift is needed in one of the arm and it is achieved by adjusting the optical path difference between the two arms. So one light travels from A to B, a negative 90° nonreciprocal and a positive 90° reciprocal phase shift cancel each other. The two beams are eventually in phase to have constructive interference at B and propagate out without much loss. For back reflected light entering into B, the nonreciprocal phase shift changes its sign i.e. positive 90°. This is added with a positive 90° reciprocal phase shift to a total of a 180° shift. Hence no output is coupled from A due to destructive interference.

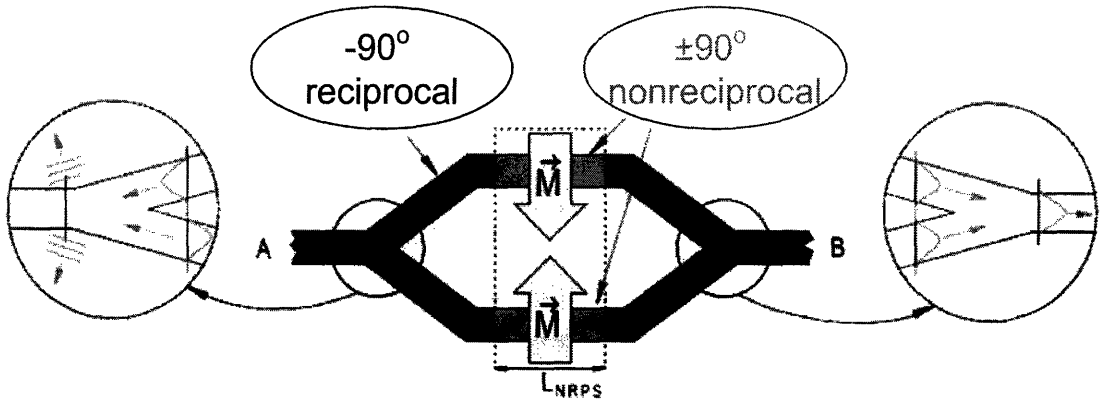


Figure 3.9 Working principle of Mach-Zehnder interferometer waveguide isolator. (Graph based on [31])

Different proposals for Mach-Zehnder type isolator have been put forward by many researchers [30, 32, 33]. Figure 3.10 shows a schematic structure of an isolator from the work by Mizumoto *et al.* [32]. The two arms of the interferometer are based on rib waveguides. In order to align the in-plane magnetization and effectively produce the nonreciprocal phase shift, the magnetic fields generated by an electric current flowing in an Au electrode were applied in the opposite directions in the two nonreciprocal phase shifters transversely to the propagation direction. The rare earth iron garnet $(LuNdBi)_3(FeA1)_5O_{12}$ was LPE grown on GGG substrate as guiding layer. Faraday rotation obtained at $\lambda$= 1.31 μm was 600°/cm and the final device length was about 12 mm.

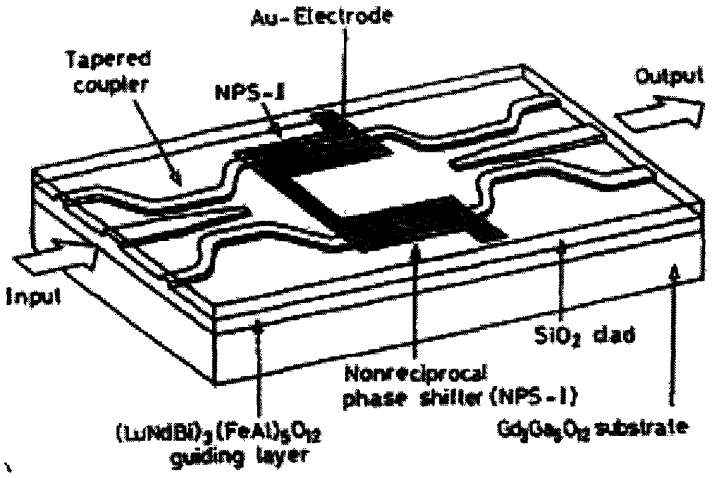


Figure 3.10 Structure of interferometric waveguide isolator employing the non reciprocal phase shift [32].

-19 dB of optical isolation in Mach-Zehnder device has been demonstrated by Fujita *et al.* [34]. A bismuth- lutetium-, and neodymium-iron garnet film $(Bi,Lu,Nd)_3(Fe,Al)_5,O_{12}$ was grown by LPE on GGG substrate. The Mach-Zehnder device was patterned by a photolithographic direct laser writing system. The total length of the fabricated waveguide isolator is 8.0mm with excess loss of 2 dB. With higher Faraday rotation materials or double-layered garnets can further reduce the device length. To achieve a large phase shift $\Delta\beta$, double layer garnet films with opposite Faraday rotation were prepared where the boundary between layers was located close to the maximum of $|H_y|^2$ [35]. Figure 3.11 shows the calculated nonreciprocal phase shift of the $TM_0$ mode for a double and a single layer. For the double layer the maximum of $\Delta\beta$ is about 2.5 times larger than that for the single layer. In addition, at a larger film thickness the dependence of $\Delta\beta$ on the film thickness is weaker. These properties are important for practical applications. To reduce the temperature dependence of the positive Faraday-rotation, a paramagnetic bottom layer with negligible Faraday-rotation was used [36].

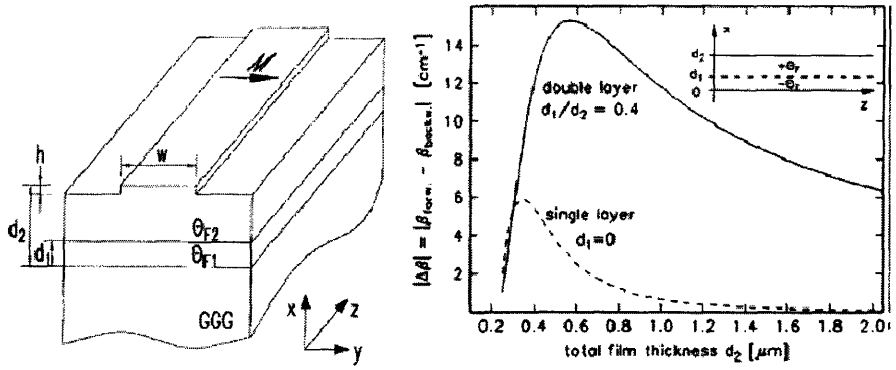


Figure 3.11 Calculated nonreciprocal $TM_0$ mode phase shift for a double and a single layer planar waveguide with a faraday rotation of 1152°/cm at wavelength of $\lambda = 1.3$ μm. The refractive indices are $n_c = 1$, $n_f = 2.33$ and $n_s = 1.95$ for the cover, film and substrate, respectively. [35]

Most MZI isolators developed have nonreciprocal components in both interferometer arms so that the nonreciprocal effects add up. There are also designs with one nonreciprocal arm with length twice as long as that for isolator with two nonreciprocal arms [31, 37]. The main advantage of this design is that the whole device is magnetized in just one direction so that one external bias magnetic field would be enough to magnetize the isolator. Figure 3.12 shows the basic geometry of this unidirectional magnetized MZI isolator. In order to have a well defined length for nonreciprocal phase shifters, Bahlmann *et al.* [31] replaced the magnetic layer by dielectric film for the rest reciprocal part. After masking the nonreciprocal waveguide section, the magnetic garnet film was removed by dry etching and this region was filled with a dielectric layer of the same refractive index like titanium dioxide.

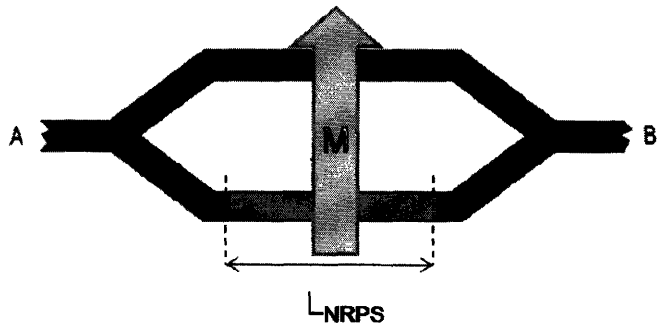


Figure 3.12 Basic geometry of Mach-Zehnder interferometer with one nonreciprocal arm. (Graph based on [31])

Figure 3.13 shows another design of unidirectional magnetized MZI isolator by Yokoi *et al.* [37]. The nonreciprocal phase shifter is a three-layer slab waveguide with the structure of upper cladding–garent (Ce:YIG)–Substrate. When the upper cladding layer of arm 1 and that of arm 2 are the same, the nonreciprocal phase shifts produced in the two arms are identical and hence cancel each other. When the layer structures of arms 1 and 2 are different, there will be propagation constant difference between them. The upper cladding layer in arm 1 is high-k dielectric materials, e.g. $HfO_2$ and that for arm 2 can be air, $SiO_2$ or even photo–sensitive materials whose refractive index can be adjusted under UV irradiation for tuning purpose. With a total device length of 2 mm, an isolation ratio of approximately 9.9 dB was obtained in the unidirectional magnetic field.

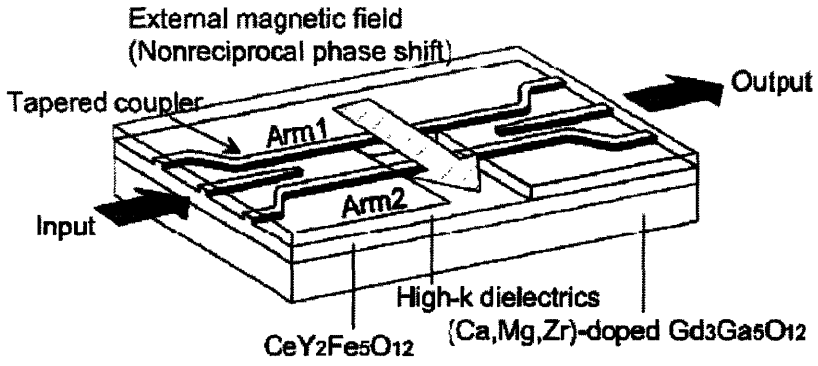


Figure 3.13 Schematic diagram of an interferometric optical isolator with distinct layer structures that employs a unidirectional magnetization [37].

### 3.3.2 TE Mode Nonreciprocal Phase Shift Isolators

Most of the III/V semiconductor lasers are TE polarized. Thus, it is essential to realize integrated isolators for TE modes, for which the change of the Faraday rotation must take place along a vertical plane. The reciprocal phase shift of the TE mode was first predicted by Popkov *et al.* [38], using a rib waveguide parallel to stripe domains. Fehndrich *et al.* [39] did the experimental measurement of the nonreciprocal phase shift of the TE mode of a rib waveguide using stripe domain lattice parallel to the waveguide having a period equal to the rib width as shown in Figure 3.14a. The arrangement of domains perpendicular to the waveguide is used as reference for calculation (right part of Figure 3.14b) because this geometry does not induce a nonreciprocal effect. A phase shift of

$|\Delta\beta| = (0.8 \pm 0.2)$ cm$^{-1}$ was observed, which was about half of the calculated one. The probable reasons might be ununiformity of domain structure and defects along the rib.

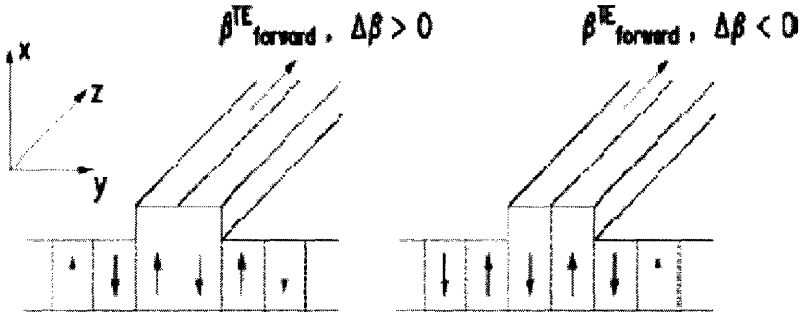


(a)

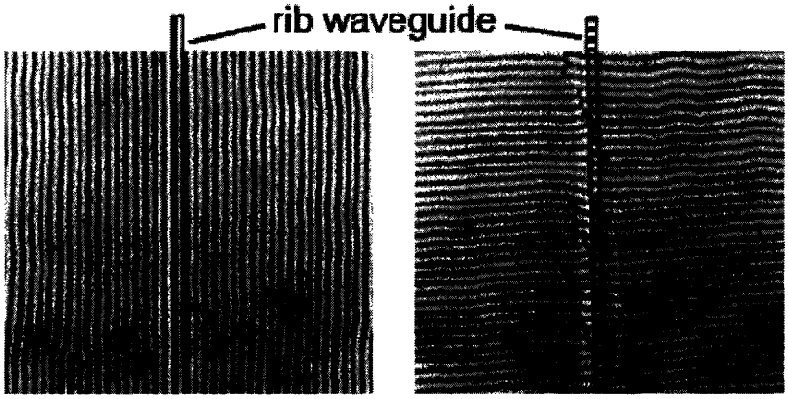


(b)

Figure 3.14 (a) Principle of the nonreciprocal TE mode phase shift using a stripe domain lattice (b) experimental arrangements that domain parallel or perpendicular to the rib [39].

The reciprocal phase shift can be enhanced if a vertical compensation wall is used instead of a domain wall at the waveguide center [40, 41]. The compensation wall (Figure 3.15) is fixed and does not change position by applying an external magnetic field, so the predicated phase shift is higher, $|\Delta\beta|$ of 2.9 cm$^{-1}$, if the compensation wall is located at the rib center from the work by Wilkens *et al.* [41]. However a rather small value of 0.7±0.2 cm$^{-1}$ was observed, which might be due to variation of the compensation wall along the rib (Figure 3.15b) and the irregularity of cross section of the waveguide. An isolator concept for TE modes based on this configuration is presented by Bahlmann *et al.*

[42]. A schematic illustration of the cross section of the isolator is shown in Figure 3.16. The sign of the Faraday rotation can be changed in a rectangular area by a special annealing process. The boundary is designated as a compensation wall. Since the Faraday rotation switches in one arm from positive to negative and in the other arm from negative to positive, the nonreciprocal phase shifts add. To obtain the desired performance, the interferometer arms must be in phase in the forward direction and $\pi$ out of phase in backward direction. This is achieved by a local change in the propagation constant as a result of modified waveguide thickness. The estimated arm lengths are comparable to those of TM-mode isolators.

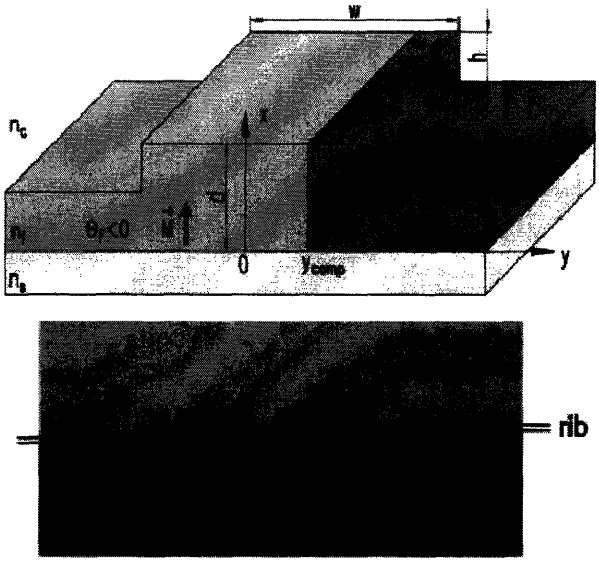


Figure 3.15 (a) The principle of the nonreciprocal TE mode phase shift using a compensation wall (CW) located inside the rib waveguide (b) Photograph of a compensation wall and a rib waveguide. The CW is visible by the Faraday contrast and the rib waveguide is marked by the two parallel lines [41].

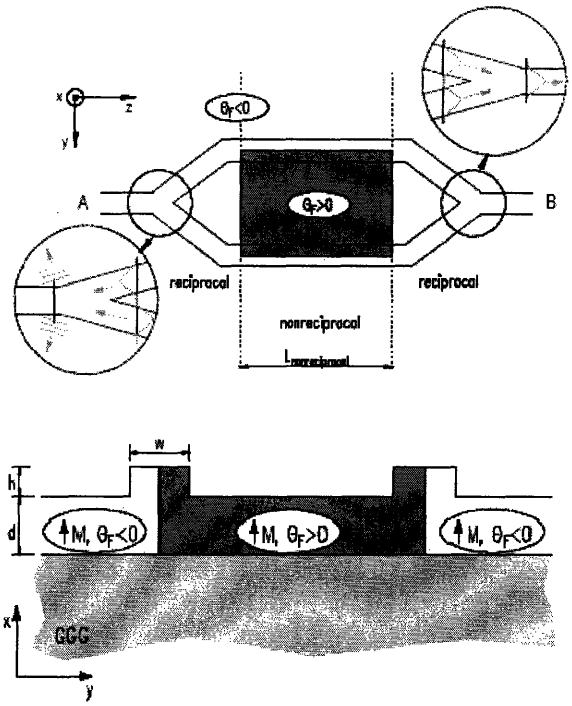


Figure 3.16 Top view (top) and cross-section view (bottom) of Mach-Zehnder interferometer for TM mode by compensation wall [42].

### 3.3.3 Polarization Independent Nonreciprocal Phase Shift Isolators

Polarization independent devices are desirable for broader applications. To obtain such waveguides, discontinuities of the Faraday rotation along horizontal lines as well as along vertical lines are required. The first such concept was investigated by Zhuromskyy *et al.* [43]. This device had horizontal and vertical magnetic domain walls in two interferometric arms separately to simultaneously induce TE and TM nonreciprocal phase shifts. Three different structures, rib, square embedded and raised strip waveguide were simulated and the geometric tolerance were very tough. Fujita *et al.* [44] proposed a polarization independent isolator with geometric asymmetry. When waveguide is symmetrical with respect to the x-z plane and magnetization uniformly along the x axis, it produces no nonreciprocal phase shift for TE modes. The situation changes in an asymmetrical waveguide, but the phase shift of the TE mode is quite small compare to that of the TM mode. There are several advantages of this design: no vertical or horizontal opposing domain walls are required and fabrication process is simplified. A

theoretical discussion of four different design concepts to realize optical isolators is presented in [45]. Figure 3.17 shows structures of the phase shifter with a 90° domain, compensation wall phase shifter with inclined magnetization, two-layer phase shifter and asymmetrical waveguide phase shifter. Each of them was optimized to the structure with equal nonreciprocal phase shifts for the fundamental TE and TM modes.

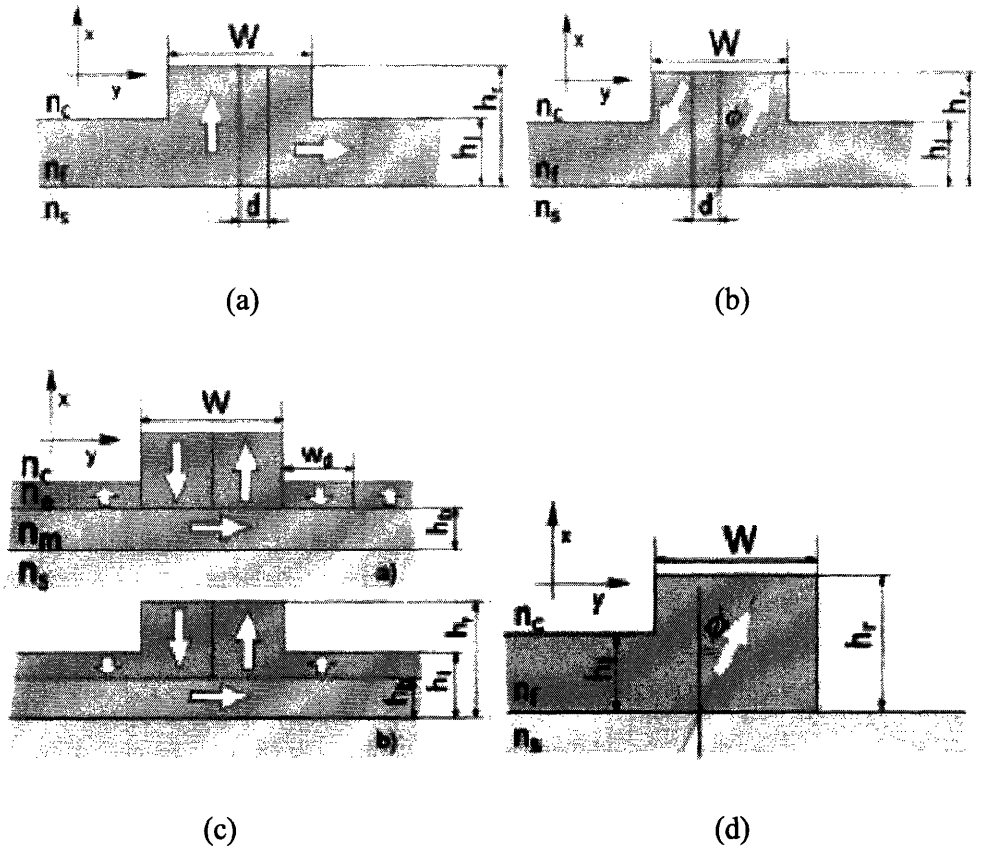


Figure 3.17 (a) Phase shifter with 90° domain wall. (b) Phase shifter with 180° compensation wall and magnetization inclined by an external magnetic field. (c) Two-layer phase shifter. (d) Asymmetrical waveguide phase shifter [45].

The most promising structure is depicted in Figure 3.17c which consists of two layers. The white arrows indicate the direction of the magnetization. The top layer supports a lattice of parallel stripe domains having a period which equals the rib width or it has a vertical compensation wall at the rib center. A nonreciprocal phase shift of $\Delta\beta$ = 40°/mm equal for both TE and TM modes was obtained for the case of the compensation wall. A Mach-Zehnder type interferometer was designed based on this configuration [45].

# 4. The Integration of Waveguide Isolators

Besides the design and fabrication difficulties in the stand-alone waveguide isolators described in the previous section, more issues arise when we want to incorporate those waveguide isolators on semiconductor substrate with other optical devices. Basically various kinds of materials need to be combined into one system using chemical or physical techniques. Difference in materials properties, i.e. mismatch in refractive index and lattice constants, leads to structural re-design and modification in fabrication processes. Though the researches on the waveguide isolators traced back to 1970s, the integration work is still limited. This section summarizes the current status of integration work, remaining issues and proposed solutions for practical integration of waveguide isolators.

## 4.1 The Hybrid Integration of Nonreciprocal Mode Conversion Isolators

Sugimoto *et al.* demonstrated the first integration of isolator on a silica-based planar circuit [17]. This type waveguide isolator resembles the bulk device, so all the auxiliary components that the bulk device has need to be integrated with the mode conversion rotator to one common substrate. Figure 4.1 is the schematic configuration of the device, which includes a 45° nonreciprocal waveguide rotator (NRWR), a thin film-type half-wave plate sheet, four thin film-type polarizers and a thin plate-type permanent magnet on a silica-based planar lightwave circuit. The NRWR was pre-prepared and then mounted upside down on terraced silicon. Four thin film-type polarizers were inserted in the grooves located on either side of the RWR chip to realize TE mode operation. To maintain the mode after rotation, a half-wave plate sheet which functioned as a 45° reciprocal rotator was inserted at the output side between the NRWR and the silicon waveguide. This whole assembly was then covered with a thin plate type magnet whose magnetic field direction was the same as that of the light propagation direction. The size of the chip was 3mm (W) x 8 mm (L) x 1 mm (T). The device has an isolation of 25 dB at $\lambda$ = 1.5 μm and an insertion loss about 3 dB. It is considered as adequate for the

isolation function in most of the optical system. The main reason for the excess loss would be the offset in the alignment between the core center positions of the NRWR and silica based waveguide.

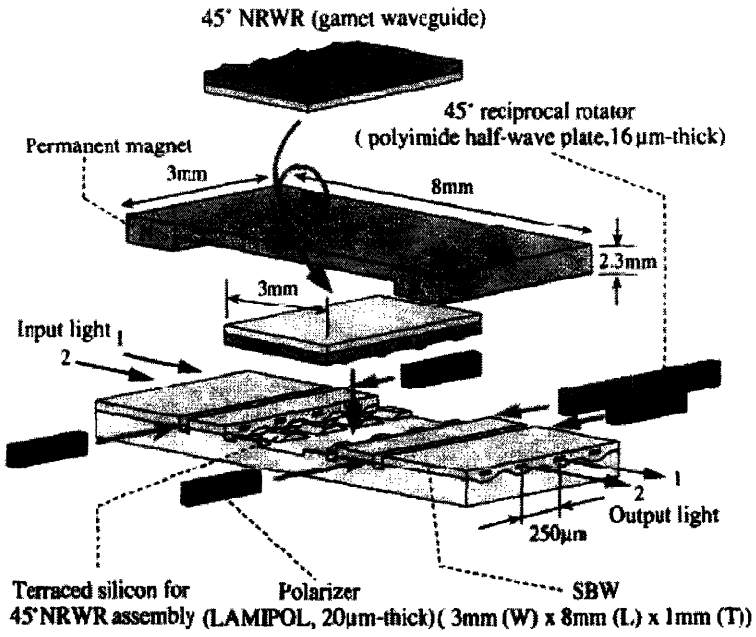


Figure 4.1 Comfiguration of a hybrid integrated waveguide isolator array fabricated on a silica-based planar lightwave circuit. The above figure and caption are from. [17]

Though the performance of this particular device fabricated can meet the isolation requirement of optical system, the complication of such assembly hindered its further development. The most stringent requirement of fabrication is the waveguide birefringence reduction as discussed in section 3.2. And the time consuming unautomated alignment between waveguides becomes another barrier. In addition, two polarizers, normally set at 45° to each other is required using faraday effect for optical isolation. It is not obvious to have difficult 45° selectivity waveguide polarizer. So most demonstrations of optical isolation using Faraday effect used external polarizers or etched slots in base to insert plate polarizers as demonstrated in this work. As an alternative to using two rotated polarizers, Huang *et al.* [46] combines functionalities of the polarizers and half-wave plate with an asymmetric rib waveguide. They fabricated a GaAs/AlGaAs waveguide using an anisotropic wet etch to obtain an angled facet on one side of the waveguide as

shown in Figure 4.2. In such a structure, a solely TE (or TM) polarization results in beating and periodical rotation between TE and TM modes. This rotation is reciprocal. Hutchings described a schematic as blueprint for an integrated isolator of such kind utilizing reciprocal polarization rotation [47].

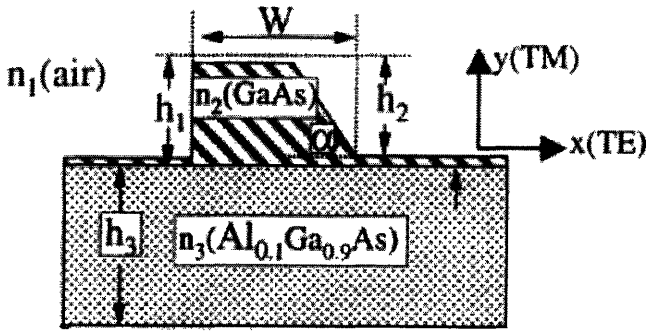


Figure 4.2 Asymmetrical rib waveguide which provides a reciprocal polarization rotation [46].

## 4.2 Designs for Continuous Core Propagation

Most waveguide isolators discussed so far have thin film garnet materials as core propagation media. For this case, the optical isolators are fabricated separately and then integrated with other optical devices such as laser diode. The pre-fabricated isolator is bonded to the common substrate with laser diode. Such integration requires accurate alignment between the two cores to minimize coupling loss. One of the main purposes for integration is to eliminate alignment process for isolator and reduce the assembly cost. Hence this integration method will not achieve true system integration as desired. Furthermore, as Hutchings pointed out, "the function of isolators is to prevent stray reflections back-propagating and therefore the isolator itself should not cause back-reflections" [47]. Reflection would occur whenever light travels through different materials. Anti-reflective coating is used in bulk isolator to prevent reflection. But for integrated system, it is important to reduce the reflection between different devices especially when the mismatch of refractive index is large. So the big difference between the refractive index of semiconductors and garnets increases the reflection and coupling losses at the interface. The above reasons largely limit the element hybrid approach.

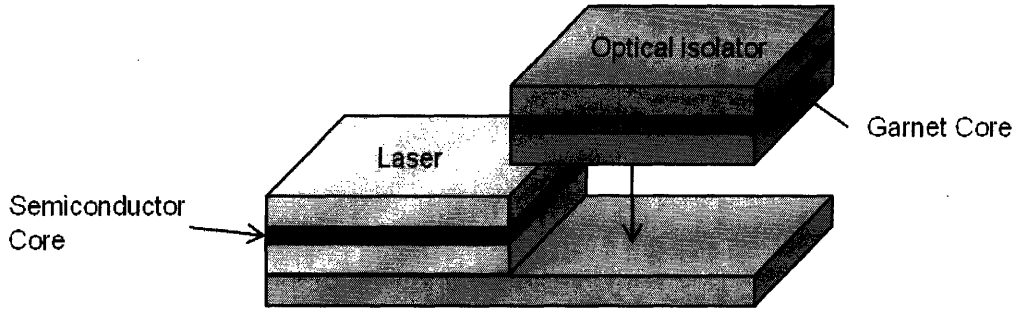


Figure 4.3 Wafer bonding of isolator to semiconductor substrate (After Sakurai *et al.* [48])

Magneto-optic cladding approach becomes attractive because semiconductor can serve as core materials for isolator and hence continuous core propagation is achieved. This provides higher compatibility with other semiconductor optical devices and facilitates the future monolithic integration of isolator as utilizing the common substrate would be possible. For nonreciprocal mode conversion isolator, the quasi phase matching mechanism utilizes magneto-optic garnets as cladding layer, which has been introduced in previous section. Yokoi and Mizumoto first proposed the nonreciprocal phase shift isolator with semiconductor guiding layer [49]. This isolator also employed the Mach-Zehnder interferometer configuration with nonreciprocal phase shifter in two arms same as described in section 3.3, except that the magnetic garnets served as upper cladding layer by direct wafer bonding technique (Figure 4.4). In this proposal, garnet was bonded on GaInAsP/InP structure and the contribution of magnetic garnet to the nonreciprocal phase shift was weak as the lower cladding materials (InP) had a higher refractive index than garnets. The first nonreciprocal phase shifter of this kind was fabricated with a Ce:YIG/GaInAsP/InP structure and an isolation ratio of 4.9 dB was achieved at wavelength of 1.55 μm [50]. The evanescent field penetration into garnets could be improved by replacing InP with materials having refractive index lower than garnet. To achieve larger nonreciprocal phase shift and shorter device length, garnet on SOI (silicon on insulator) magneto-optic waveguide was fabricated by wafer bonding [51, 52]. Higher compatibility with other optical devices is expected since SOI becomes an increasingly popular platform for optical integration. From the comparison between the waveguides with three different layer structures garnet/SOI, air/garnet/garnet substrate, garnet/GaAsInP/InP, two groups reached the same conclusion that garnet/SOI is the most

promising structure among the three because low refractive index material $SiO_2$ is used as the lower cladding layer which enhance the evanescent field penetrating into the upper garnet cladding layer [52]. Instead of using magnetic garnet as upper cladding layer, another configuration was proposed, which has air/$TiO_2$/Ce:YIG structure with $TiO_2$ as guiding layer [53]. Double layer $TiO_2$/garnet serving as guiding layer was also investigated and it improved the performance compared to single guiding layer.

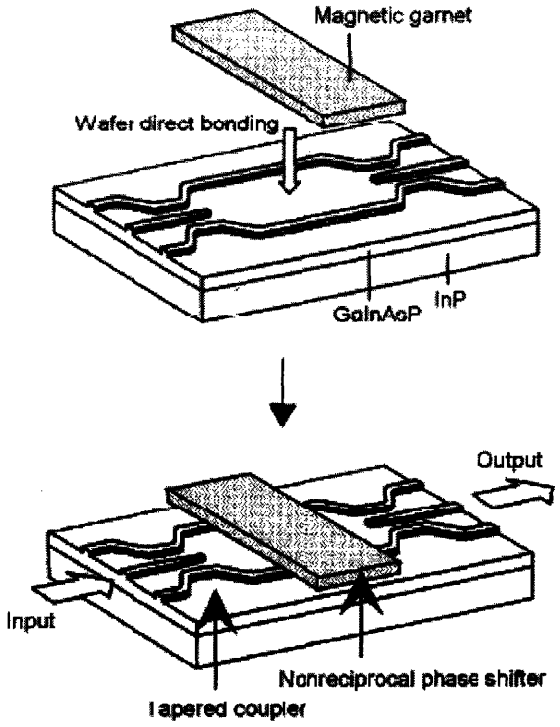


Figure 4.4 Schematic illustration of integrated optical isolator fabricated by wafer direct bonding technique [49].

## 4.3 Monolithic Integration of Optical Isolators with Laser Diode

Mizumoto proposed the waveguide optical isolator integration with laser diode since the isolator has GaInAsP guiding layer, which enhance the compatibility with other semiconductor devices [54]. For proof of concept, a preliminary Fabry-Perot laser integrated with an optical passive waveguide was designed and fabricated using the wafer grown by selective-area growth technique [48]. The schematic design and layer structure are shown in Figure 4.5. By masking a portion of the substrate surface with a dielectric

such as $SiO_2$ before epitaxial growth, the semiconductor layer, whose composition is locally modified to become suitable for use in active and passive devices, is grown in a single growth step [55]. Standard photolithography process is used to define the pattern of a laser stripe and a passive waveguide for an optical isolator. Both vertical and horizontal alignment can be achieved between two devices. Figure 4.6 shows one of the mirror facets for a Fabry-Perot laser formed by a narrow groove using focused ion beam (FIB) etching in the transition region between the active and the passive regions. In order to form vertical mirror facet, the wafer normal is tilted with respect to the ion beam. Several excess loss mechanism need to be taken care of in this design: the diffraction loss in the air gap, the coupling loss at the inclined facet, the reflection caused by refractive index difference and the propagation loss in the passive waveguide. An estimation of 6.5 dB excess loss is estimated, which can be reduced by careful design of the system and tighter control of fabrication process.

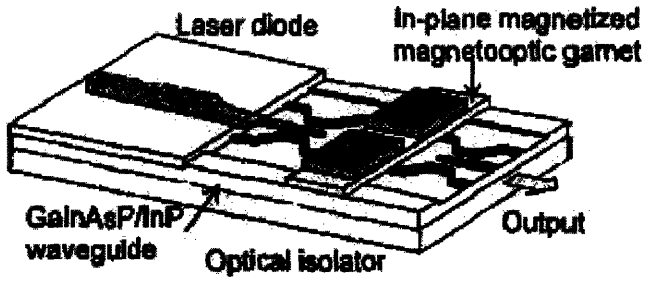


(a)

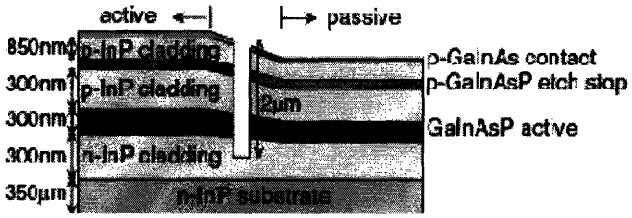


(b)

Figure 4.5 (a) Schematic drawing of an optical isolator with a semiconductor laser [54]. (b) Layer structure of the selectively grown wafer [48].

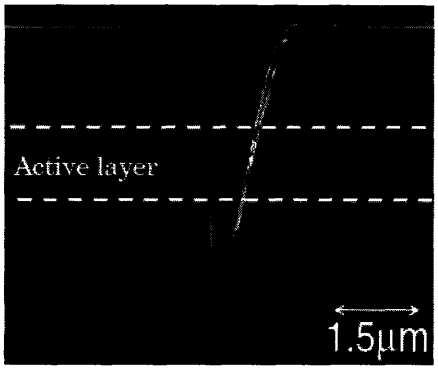


Figure 4.6 Cross-section SEM image of etched groove fabricated by FIB [58].

## 4.4 Materials Issues Related to Integration Techniques

The critical active element in optical isolator garnet materials are difficult to integrate with semiconductors due to high thermal budge usually required obtaining the garnet crystal structure. Current isolator garnets cannot be integrated monolithically into a photonic integrated circuit due to the growth process of liquid phase epitaxy (LPE). To develop an effective way of integrating these two kinds of materials occupies researchers' attention for a long period of time. This section summarizes a few approaches for optical isolator integration, ranging from developing novel growth method, novel materials, to exploring the potential of existing semiconductor materials.

### 4.4.1 Wafer Direct Bonding of Garnets with Semiconductor Materials

Wafer bonding is a promising technique to integrate non growth-compatible materials. Optical isolators with magnetic garnet as upper cladding layer structure become popular for high compatibility with other semiconductor devices because they have semiconductor guiding layer which can be monolithic grown in one step. The upper cladding magnetic garnet layer of optical isolators (described in section 4.2) were fabricated by wafer-direct bonding [49-54]. Garnets have been bonded to GaInAsP/InP wafer with heat treatment at the temperature as low as 220 °C in $H_2$ ambient and showed sufficient durability against fabrication processes such as high temperature (600 °C) annealing, semiconductor wet etching and plasma process [49, 54, 56, 57]. Wafer bonding between Si and the garnet crystal GGG was also successfully achieved with the

heat treatment at 220 °C in $H_2$ ambient [58]. Izuhara *et al.* [59] also studied the bonding between Bi:YIG and Si, GaAs, InP substrate. The Bi:YIG thin film was separated from GGG substrate by crystal ion slicing technique [60, 61]. Wafer surfaces need treatment to render the surface hydrophilic prior to bonding. Bonding was performed at 200 °C for all the three substrates to obtain a bonding strength comparable to Si-to-Si bonding. Due to the differential thermal expansion of materials, heterogeneous structure would suffer thermal stress. Above 400 °C, the bonded area starts to decrease rapidly in the case of Si. However, bonding to InP and GaAs could persist to higher temperatures, 700 °C [59]. Wafer bonding technique was also utilized to hybrid integrate pre-fabricated isolator with laser diode [62] (as shown in Figure 4.7). Successful bonding between GaInAsP and GGG was achieved at 220 °C without degradation of the laser diode.

The quality of horizontal interface after bonding is important for low-loss optical guiding. The smoothness at the sub-wavelength level is difficult to achieve by wafer bonding method. It makes process very complicated if more components are to be bonded without automated alignment technique. However, it is still the most promising technique for hybrid integration of non-compatible materials.

### 4.4.2 Epitaxial Growth of Garnets on Semiconductor Materials

Some semiconductor friendly processes have been developed for garnet film growth [63-69]. These films have in-plane magnetization and small coercive fields that are desirable for waveguide magneto-optic devices. YIG films were fabricated on MgO substrate by RF sputtering method [63, 64]. MgO is good optical cladding that can be deposited by sputtering onto semiconductors. In precious study, an MgO buffer layer was proved to be able to protect semiconductor substrates during subsequent thermal processes at over 850 °C [70]. $SiO_2$ and $Si_3N_4$ films were demonstrated to be noncompliant with YIG, as stress fractured these films [66]. An improved technique which involved a multi-target reactive RF sputtering system, partial pressure differentials and rapid thermal annealing produced better results than conventional gas feed-through technique [64, 65]. The deposition rates are higher and more significantly with a rapid thermal annealing (RTA) in $O_2$ instead of air, 15 seconds annealing at 750 °C is enough to achieve full

crystallization, a big improvement compared with conventional method of 3 hours at 800 °C [63]. Growth methods for Bi-YIG and Ce-YIG films onto semiconductor platforms by various techniques have also been developed [63, 67, 68]. Stadler *et al.* found that using metal-organic chemical vapor deposition (MOCVD), large amount of Ce (up to 54%) could be incorporated into the garnet structure because of the nonequilibrium nature of the technique. Faraday rotation achieved in MOCVD-grown garnet exceeds that of Bi-YIG by LPE method [67]. Growth parameters need to be further optimized to enhance the integrity of the film and annealing temperature need to be further reduced to be compatible with semiconductor processes.

### 4.4.3 Novel Magneto-optic Materials Compatible with Semiconductor Materials

Some groups are looking at novel non-garnet materials that are semiconductor compatible, transparent in telecommunication wavelength and have Faraday effect comparable to garnet. Transition-metal-doped perovskites of the form ($ABO_3$) are being studied [71]. Pure perovskites generally are weak ferromagnetic, but doping with Fe iron can induces ferromagnetism in the oxide. Fe doped $BaTiO_3$ ($BaTi_{1-x}Fe_xO_3$) was chosen because it grows epitaxially on MgO substrate by pulsed laser deposition. However, the increasing Fe content also increases the optical absorption. The magneto-optic figure of merit is defined as the ratio of Faraday rotation to absorption. The experiment data of $BaTi_{1-x}Fe_xO_3$ figure of merit in terms of x is shown in Figure 4.7 [71]. $BaTi_{0.8}Fe_{0.2}O_3$ has the highest figure of merit of 3.7° /dB and the calculated absorption corresponding to a rotation of 45° is 12.1 dB. The optical loss is high for practical application so ferromagnetic materials with lower optical absorption are desirable.

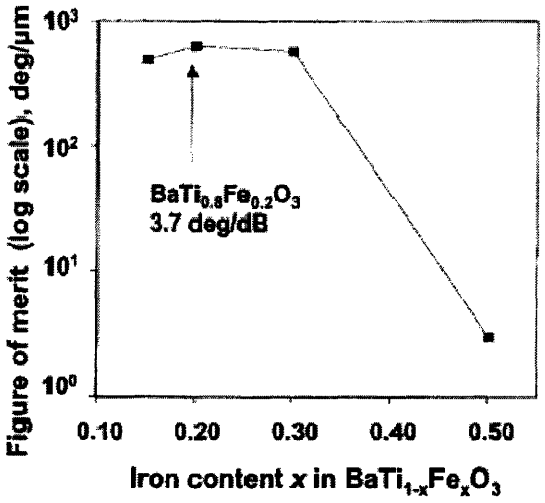


Figure 4.7 Magneto-optic figure of merit in $BaTi_{1-x}Fe_xO_3$ as a function of Fe content x [71].

### 4.4.4 Doped and Dilute Semiconductor Materials

Due to the difficulties in using magneto-optical materials for integrated isolators, researchers start to explore magneto-optic effect of the materials used in semiconductor chips. The Verdet coefficient of semiconductors mainly comes from interband contribution, which is resonant at the band-edge. However, the values of Verdet constants are small for binary semiconductors, typically range from $10^{-5} - 10^{-4}$ $radA^{-1}$. For the case of GaAs, it would require a current of the order of 10 A flowing in conductor a few 10 μm to obtain a $\pi/4$ rotation [47].

Verdet constant can be increased by introducing ferromagnetic elements into the semiconductor. MnAs nanoclusters in GaAs (GaAs:MnAs) shows superparamagnetic properties at room temperature. GaAs:MnAs is obtained by annealing (GaMn)As at 500 – 600 °C has a rotation angle of 0.2°/μm at wavelength 980 nm and at field strength of 2000 Oe, which yields 225 μm length for 45° rotation [72]. It has excellent compatibility with nonmagnetic III-V heterostructures with a large magneto-optical effect and hence monolithically integrated with semiconductor laser diodes can be considered. However, absorption coefficient of the materials is still far beyond the criterion for practical application. The absorption and magneto-optical properties of GaAs: MnAs are strongly dependent on its cluster size and [GaAs: MnAs]/AlAs superlattices structure is found to

provide better control of the MnAs nanocluster size and hence reduce the optical absorption [73]. At the telecommunication wavelength $\lambda$=1550 nm, waveguide Faraday rotation was demonstrated in an InP waveguide with Fe doping [74]. The waveguides consisted of a 0.5 μm $In_{0.71}Ga_{0.29}As_{0.628}P_{0.372}$ core lattice with a 1.0 μm InP cladding on both top and bottom. The entire structure was Fe doped. At a magnetic field of 1 T, the figure of merit of 23°/dB was obtained. The magneto-optical performance looks promising for optical isolator application, but the magnetic field of 1 T is difficult to achieve in an integrated system.

Dilute magnetic semiconductors normally with a substitution of the group II element with Mn or Fe could significantly increase Verdet constant. In particular, mode conversion has been demonstrated in $Cd_{1-x}Mn_xTe$ waveguide which was epitaxially grown on GaAs substrate [75,76]. The waveguide showed an optical loss below 1 dB/cm, and a magneto-optical figure of merit 200°/dB/kG at $\lambda$=730 nm. A recent development in growth of a graded-refractive-index layer (by varying x, the Mn concentration, with thickness) at a waveguide boundary has reduced the mode phase mismatch in the waveguide, and a mode conversion ratio 98% ± 2% under a magnetic field of 5kG was achieved allowing the prospect of practical devices [76].

# 5. Competitive and Market Analysis

Previous sections provide overview about development history and current status of integrated magneto-optical isolators. To access the commercialization potential of a technology, the knowledge of the development trend and status of competitive technology is essential as well. One category of competition rises from the technology which tries to utilize other means rather than the Faraday effect to provide optical isolation; the other comes from the technology that tries to get rid of using optical isolator all together by realizing reflection resistant devices.

## 5.1 Competitive Waveguide Optical Isolators

### 5.1.1 Nonreciprocal Loss Optical Isolators

A novel concept for integrating optical isolators for better compatibility with III-V semiconductor materials was proposed by Takenaka and Nakano [77] and by Zaets and Ando [78] in 1999. This optical waveguide isolator basically is a semiconductor optical amplifier (SOA) with a ferromagnetic metal contact very close to the active region. Figure 5.1 shows a schematic layout of the waveguide optical isolator for TM mode. To operate the device, an external magnetic field is applied so that the ferromagnetic metal layer is magnetized transverse to the light propagation direction. This induces a non-reciprocal shift of the complex refractive index of TM mode due to MO Kerr effect in the ferromagnetic transition metals. This phenomenon is called nonreciprocal loss that the propagation loss of light is larger in backward than in forward direction [77, 78]. Isolation behavior is achieved by the difference in optical propagation loss in the opposite directions. The amount of the MO Kerr effect is related to the amount of guided light that overlaps the lossy MO layer. The SOA compensates for the forward propagation loss that the net loss for forward propagation will be zero. Under these conditions, the device is able to act as an optical isolator.

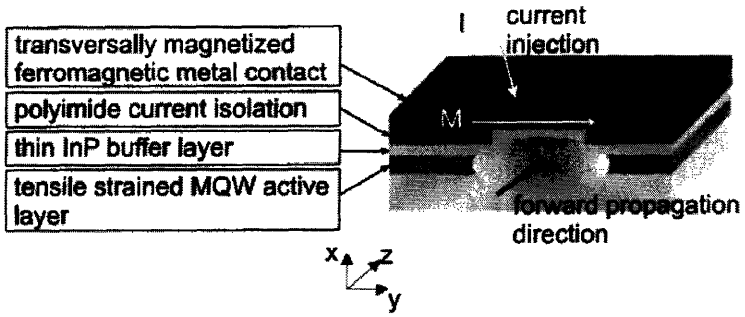


Figure 5.1 Schematic layout of a two-dimensional cross section of the nonreciprocal loss waveguide optical isolator [79].

The first example of the nonreciprocal loss isolator was reported by Vanwoleghem et al. [80, 81]. The device consists of an InGaAlAs/InP MQW active layer with a ferromagnetic CoFe layer and operates in 1.3 μm TM mode. According to Postava *et al.* [79], two important factors are essential to experimental success: a high quality ferromagnetic MO metal-semiconductor interface and a high quality active semiconductor gain region. In this case, the MO metal needs to fulfill three functions: to be a good ohmic contact for SOA, to be a good permanent magnet in the transverse direction, and to possess a strong MO constant in telecommunication wavelength range of 1300-1600 nm. MnAs has been used instead of ordinary ferromagnetic metals (Fe [83] or $Co_{50}Fe_{50}$ [81]) for lower contact resistance with SOA [82]. Though the Currie temperature of MnAs is a little low at about 40 °C, it can be used in photonic circuit because such circuits are generally used at controlled temperature to operate laser diode stably. TE mode waveguide isolators have also been experimentally demonstrated by aligning the magnetization vector of the magneto-optical material (Fe) parallel to the magnetic field of the TE mode light, i.e. perpendicular to the waveguide [82, 83, 84]. The best isolation ratio (nonreciprocal loss) reported so far are 14.7dB/mm for TE mode for 1.3 μm wavelength [84] and 9.9 dB/mm for 1.55 μm wavelength [81]. Right now the forward propagation loss, about 7.1 dB/mm is still way beyond the limit for practical application. This device requires current injection for active operation, but it is promising for semiconductor waveguide optical isolators monolithically integrated with laser diodes if insertion loss can be reduced below 1 dB/mm.

### 5.1.2 Non Magneto-Optic Isolators

The simplest idea of optical isolation is using cascaded coupler as depicted in Figure 5.2. A planar optical isolator is formed within the silicon surface layer of an SOI structure [85]. A forward-directed signal is applied to an input section of the isolator and thereafter propagates through a coupling region into an output waveguide section. A reflected signal enters via the output waveguide section and is thereafter coupled into the waveguide, where it functions to couple only a small amount of the reflected signal into the input. Therefore, a nonreciprocal isolation is achieved. By using N way directional couplers (with one output waveguide, one input waveguide and N-1 terminated isolating waveguides) and cascading a number of such planar structures, increased isolation can be achieved. This isolation scheme is simple and easily integrated with any semiconductor system. However, to have a high isolation ratio for practical application, the device is going to be long and insertion loss of the coupler will scale with the waveguide length. Hence there are no commercialized devices yet.

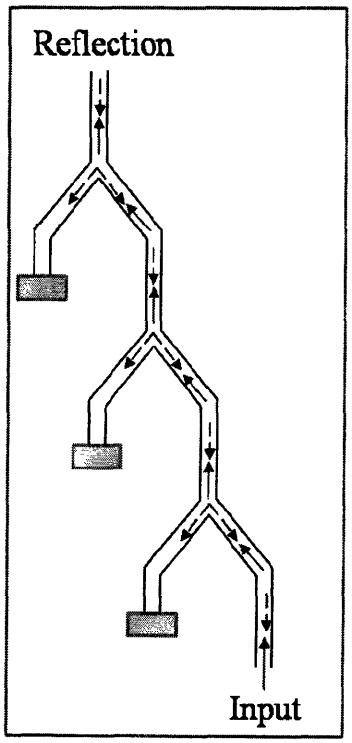


Figure 5.2 Nonreciprocal isolator by cascaded directional coupler (after [85]).

Another novel ideal to implement waveguide-type isolators in III/V materials was proposed in 2005 [86]. This device consists of a single-sideband electrooptic modulator where traveling electrical waves make the transmission direction-dependent. Traveling waves consisting of electrical ac signals are needed to break the symmetry between the propagation directions and thereby configure it to behave as an optical isolator. As shown in Figure 5.3, the single-sideband electrooptic modulator contains two traveling wave Mach-Zehnder modulators with electrode length L. Two of these modulators form a Mach-Zehnder superstructure. This superstructure has quadrature control electrodes in both arms for active phase control. Isolation of 30 dB was obtained with excess insertion loss of 8 dB [86].

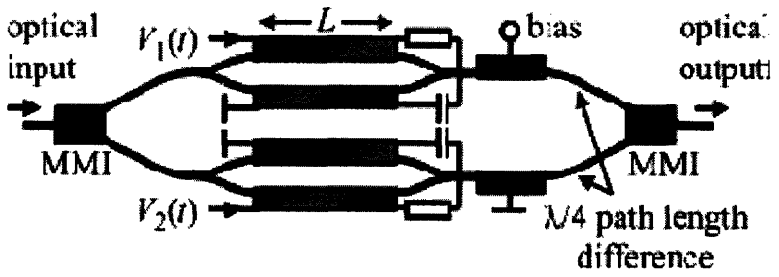


Figure 5.3 Traveling-wave single-sideband (TW-SSB) isolator [86].

## 5.2 Market Analysis

### 5.2.1 US Patents Related to Integrated Optical Isolators

According to my personal statistics, there are 14 US patents (Table 1) directly related to magneto-optical isolator in waveguide or integrated form and 6 US patents (Table 2) for non-magnetic waveguide optical isolator.

Structure Related Patents

| | Year | Patent # | Title | Assignee |
|---|---|---|---|---|
| 1 | 2007 | 5598492 | Metal-ferromagnetic optical waveguide isolator | US Department of the Army |
| 2 | 2006 | 7043100 | Polarization independent waveguide optical isolator and circulator | E. I. du Pont de Nemours and Company, US |
| 3 | 2006 | 7130494 | Magnetically active semiconductor waveguides for optoelectronic integration | MIT |
| 4 | 2005 | 6943932 | Waveguide mach-zehnder optical isolator utilizing transverse magneto-optical phase shift | Columbia University |
| 5 | 2005 | 20050089258 | Integrated optical isolator | Korea Institute of Science and Technology |
| 6 | 2005 | 20050094923 | Integrated optical isolator using multi-mode interference structure | Korea Institute of Science and Technology |
| 7 | 2003 | 6535656 | Planar-type polarization independent optical isolator | Corning Incorporated |
| 8 | 1992 | 5078512 | Unidirectional mode converter and optical isolator using same | Agency of industrial science &Technology, ministry of international trade & industry, Japan |
| 9 | 1992 | 5101469 | Light isolator of waveguide type | Canon Kabushiki Kaisha |
| 10 | 1991 | 5058971 | Planar optical isolator | US Philips Corp. |
| 11 | 1991 | 5031983 | Apparatus comprising a waveguide magneto-optic isolator | AT&T Bell Lab |

Materials Related Patents

| | Year | Patent # | Title | Assignee |
|---|---|---|---|---|
| 1 | 2006 | 7006289 | Magnetooptical isolator material | MIT |
| 2 | 2006 | 7102171 | Magnetic semiconductor material and method for preparation thereof | Japan Science and Technology Corporation |
| 3 | 2002 | 6348165 | Semiconductor magneto-optical material | Agency of industrial science &Technology, ministry of international trade & industry, Japan |

Table 1 US patents related to integrated magneto-optical waveguide isolators

| | Year | Patent # | Title | Assignee |
|---|---|---|---|---|
| 1 | 2007 | 7164823 | Optical isolator using photonic crystal | Samsung Electronics Co., Ltd |
| 2 | 2007 | 7228023 | Planar non-magnetic optical isolator | Intel Corporation |
| 3 | 2006 | 7113676 | Planar waveguide optical isolator in thin silicon-on-isolator (SOI) structure | Sioptical Inc. |
| 4 | 2001 | 6208795 | Optical waveguide isolator | Sugimura International Patent & Trademark Agency Bureau |
| 5 | 1999 | 5901258 | Waveguide-type optical isolator and method for making the same | NEC Corporation |
| 6 | 1994 | 5463705 | Optical waveguide isolation | IBM |

Table 2 US patents related to non-magnetic integrated optical isolators

In Table 1, among the fourteen patents, eleven of them are structure related and three are related to novel non-garnet materials compatible with semiconductor for integration purpose. Before the year 2000, the patents are based on nonreciprocal mode conversion type and after 2000, all are nonreciprocal phase shifted isolator. As discussed in section 3, the nonreciprocal phase shifted isolator does not have stringent fabrication margins and would be promising for industrial manufacturing.

| | | Total | Industry | University & Institute | Gov/Agency |
|---|---|---|---|---|---|
| Magneto-optical isolator | Structural | 11 | 5 | 4 | 2 |
| | Material | 3 | 1 | 1 | 1 |
| | Total | 14 | 6 | 5 | 3 |
| Non-magnetic isolator | Total | 6 | 6 | 0 | 0 |

Table 3 Statistics on patent holders.

From Table 3, we can see that industry holds more than half of the patents (12 out of 20 ~ 60%) and the rest patents go to universities and government or government agency. Companies from Korea, Japan and the US are leading in this field, including E. I. du Pont de Nemours and Company, Corning Inc., Canon Kabushiki Kaisha, US Philips

Corp., Japan Science and Technology Corp., Sumsung, Intel, Sioptical Inc., NEC, and IBM. Obviously companies that are interested in the integrated optical isolators wouldn't limit to the list above.

Besides the two categories of magneto-optical waveguide isolators (nonreciprocal mode conversion and nonreciprocal phase shift), there are a few more non-magnetic waveguide isolators structures as described in section 5.1 as well as list in Table 2. However, up to date there is no commercial version available. Among all these structures, it is still not clear which one will be successfully integrated with semiconductor devices and get commercialized first with adequate performance and reasonable cost level.

### 5.2.2 Emerging of Isolator-free Technology

There is a special kind of competition that is the isolator-free laser technology, which ultimately competes both in laser and isolator market with existing products. Since 2005, there have been isolator-free laser product releases with different speeds for telecommunication applications. Table 4 below provides a summary and details are in Ref [87, 88].

| **Eblana Photonics (Ireland)** | Speed | Mode | Price | Application/Temp |
|---|---|---|---|---|
| 2005 | 2.5Gb/s | Single mode | $19.00 | Ethernet, SONET, Fiber Channel (0-85 °C) |
| 2006 | 3.125 Gb/s × 4 | Single mode | — | Ethernet LX4, (0-85°C) |
| 2006 | 4 Gb/s | Single mode | — | Fiber Channel (0-85°C) |
| 2007 | 10Gb/s | Single mode | — | Ethernet, Fiber Channel (-40 - 85°C) |
| | | | | |
| **Corning Lasertron, Inc. (US)** | Speed | Mode | Price | Application |
| 2005 | 2.5Gb/s | Singal mode | — | DFB laser |

Table 4 Progress and product releases in isolator-free laser technology

In March, 2007, Oki Electric Industry Co. Ltd. Japan (OKI) achieved optical isolator free capability through a Gain Coupled DFB laser with improved tolerance of optical reflection and reduced degradation from relative intensity noise when impacted by

reflected light. With this advance, OKI conducted 25km transmission experiments over the temperature range where optical modules normally operate (0 ~ 70°C) and found that in a state where reflected light (-14dB) was forcefully applied, there was almost no degradation of reception sensitivity. This confirmed a marked improvement in tolerance to reflected light, compared to conventional index coupled DFB lasers [89]. This advance in laser technology will directly influence the demand of optical isolator and create a big impact on the existing market.

### 5.2.3 Market Opportunities and Challenges for Integrated Optical Isolator

| Year | 2001 | 2006 |
|---|---|---|
| Optical isolator market | $296.3 Million | ~300 Million |

Due the downturn in optical communication in the last five years, there is almost no increase in the overall optical isolator market according to the number given by Electronicast and customer data [90]. Majority of optical isolators are for the laser system application. Currently, lasers are either discrete devices or hybrid integrated onto a common substrate with other optical components. The monolithic integration lies only between laser and modulator, such as Electroabsorptions (E/A), Indium Phosphide (InP) and Mach-Zehnder (M-Z) modulator integration. If the laser is not yet monolithically integrated, we don't see an urgent demand for monolithic integrated isolator unless the integration would bring potential benefits: enhanced performance and functional density or cost effective solutions. With the emerging of isolator-free laser technology, it imposes more challenges on the market outlook of integrated optical isolators.

From section 3 and 4 we could see that at the current stage, utilizing magneto-optic effect in waveguide isolator can't compete with bulk device in terms of isolation performance. Due to the stringent fabrication requirement, the yield is expected to be extremely low. All of the demonstrated waveguide isolators are still in the laboratory trial and error stage that there is a lack of practical solution in manufacturing environment. Currently all the proposed integrated isolator technologies (including those non-magnetic

isolators) couldn't compete with existing bulk devices in terms of performance and cost, and that would be the reasons hindering their market penetration.

Driven by the functional and cost requirement, photonic integration or even microelectronics-optics integration are the trend in technology development. Optical circuit miniaturization causes devices more vulnerable to reflections due to the small size under high frequency operation. Therefore, besides laser, more waveguide active devices such as amplifiers, modulators would require effective optical isolation. Furthermore, laser sources integrated with CMOS circuit is one of the potential future solutions in microelectronic circuit. The new market opportunities will open up a huge demand for on-chip integration of optical isolators.

The cost of bulk optical isolator in telecommunication laser system is about 10 US dollars each on average. It is difficult to estimate the cost of integrated isolator since its cost will be incorporated with the other optical devices, i.e. laser. If monolithic integration is successful, we would expect a dramatic drop in price since manufacturing would be standard semiconductor processes and individual packaging and alignment processes will be eliminated. Integrating optical isolator on chip is a challenging task. But once successful, it won't limit to the existing $300 million bulk device market. It fulfills the requirements in the new applications mentioned above. Also it reduces the overall cost of laser system, which in turn will shift the demand of telecommunication transmitter module market.

# 6. Conclusion

In this thesis, we have examined the current development of on-chip integration of magneto-optic isolator from different aspects including structural designs in waveguide form, integration techniques and materials issues.

Bulk isolator utilizes the Faraday effect to achieve 45 ° nonreciprocal rotation of polarization as light travels through the crystal. This effect is severely degraded in waveguide format due to unavoidable phase mismatches from birefringence inherent in waveguide, mismatch in materials and growth processes. To reduce the birefringence, it imposes extremely stringent fabrication requirement which can be done in the laboratory but is difficult to achieve in manufacturing. A solution to this problem is quasi-phase-match by periodically reversing the magnetic field. There are several ways to implement this in the literature for garnet films.

A more naturally adaptable phenomenon to planar geometries, the nonreciprocal phase shifts effect is promising for integrated isolator, without stringent phase-matching requirements. TE mode propagation is yet to make a big progress before the development of viable polarization-independent waveguide isolators.

Hybrid bonding of pre-fabricated waveguide isolator onto laser diode substrate is technically doable, but it won't eliminate the alignment process or reduce the assembly cost if the process is not automated. To achieve monolithic integration, high-quality optically nonreciprocal films must find their way onto silicon or other semiconductor platforms. Wafer bonding and sputter or other deposition techniques of garnet on semiconductors are possible solutions. Development of novel non-garnet materials compatible with semiconductors is already underway. Another approach is to discover the potential in semiconductors, such as doped or diluted magnetic semiconductors. Nevertheless, there is ample space for researchers to find alternatives in materials or growth techniques.

To achieve integration, garnet core propagation waveguide have issues because the refractive index of garnet is usually much lower than that of semiconductor. It induces reflection when light propagates through different materials interfaces. Magneto-optic upper or lower cladding approach is attractive since it allows continuous propagation in semiconductor core. However, additional attention is needed to enhance the magneto-optic effect in the cladding, as there is only a small amount of light tail is interacting with the cladding layer.

Potential competitions are from other form of isolators or even isolator-free technology. Which isolation scheme will succeed in integrated system is still unclear. With the potential benefits of the integration, on-chip integrated optical isolators indeed have good market opportunities in telecommunication, high frequency optical circuit and even microelectronic-optics circuit in future.

# Reference


[1] H. R. Hulme, Proc. Roy. Soc. (London) A135, 237 (1932)

[2] W. Swindell, Polarized Light, (Halsted, New York, 1975) p.104-123.

[3] J.M. Stone, Radiation and Optics, (McGraw-Hill, New York, 1963), p. 445-6.

[4] M. Levy, "The On-Chip integration of Magnetooptic Waveguide Isolators," *IEEE Journal of Selected Topics in Quantum Electronics*, **8**, 1300, (2002).

[5] T. Matsumoto, "Polarization-Independent Isolators for Fiber Optics," *Trans. IECE Japan*, **E62**, (1979).

[6] K. Shiraishi, T. Chuzenji, and S. Kawakami, "Polarization-Independent in-line Optical Isolator with Lens-free Configuration," *J. Lightwave Technol.*, **10**, 1839, (1992).

[7] H. Dötsch, N. Bahlmann1, O. Zhuromskyy, M. Hammer, L. Wilkens, R. Gerhardt, P. Hertel, "Applications of magneto-optical waveguides in integrated optics: review," *J. Opt. Soc. Am. B*, **22**, 240,(2005).

[8] M. Gomi, K. Satoh, and M. Abe, ''Giant Faraday rotation of Ce-substituted YIG films epitaxially grown by RF sputtering,'' *Jpn. J. Appl. Phys.* 27, L1536–L1538 (1988).

[9] L. Eldada, "Advances in telecom and data come optical components," *Opt. Eng.* **40(7)**, 1165, (2001).

[10] S. L. Blank and J. W. Nielsen, ''The growth of magnetic garnets by liquid phase epitaxy,'' *J. Cryst. Growth* ., **17**, 302 (1972).

[11] J. P. Krumme, V. Doormann, and B. Strocka, ''Selected-area sputter epitaxy of iron–garnet films,'' *J. Appl. Phys.* **60**, 2065 (1986).

[12] S. Kahl and A. M. Grishin, ''Pulsed laser deposition of Y3Fe5O12 and Bi3Fe5O12 films on garnet substrates,'' *J. Appl. Phys.* **93**, 6945 (2002).

[13] M. Yamane and Y. Asahara, "Glasses for Photonics", 2000, Cambridge: Cambridge University Press.

[14] M. Lohmeyer, ''Wave-matching method for mode analysis of dielectric waveguides,'' *Opt. Quantum Electron.* **29**, 907 (1997).

[15] S. Yamamoto and T. Makimoto, ''Circuit theory for a class of anisotropic and gyrotropic thin-film optical waveguides and design of nonreciprocal devices for integrated optics,'' *J. Appl. Phys.* **45**, 882 (1974).

[16] E. Pross, W. Tolksdorf, and H. Dammann, "Yttrium iron garnet single-mode buried channel waveguides for waveguide isolators," *Appl. Phys. Lett.*, **52**, 682, (1988).

[17] N. Sugimoto, H. Terui, A. Tate, Y. Katoh, Y. Yamada, A. Sugita, A. Shibukawa, and Y. Inoue, "A hybrid integrated waveguide isolator on a silica-based planar waveguide circuit," *J. Lightwave Technol.*, **14**, 2537, (1996).

[18] A. Shibukawa and M. Kobayashi, "Optical TE-TM mode conversion in double epitaxial garnet waveguide," *Appl. Opt.* **20**, 2444 (1981)

[19] R. Wolfe, J. Hegarty, L. C. Luther, and D. L. Wood, "Single mode magneto-optic waveguide films," *Appl. Phys. Letts.*, **48**, 508, (1986).

[20] H. Dammann, E. Pross, G. Rabe, W. Tolksdorf, and M. Zinke, "Phase matching in symmetrical single-mode magneto-optic waveguides by application of stress," *Appl. Phys. Lett.*, **49**, 1755, (1986).

[21] R. Wolfe, V. J. Fratello, and M. McGlashan-Powell, "Thin-film garnet materials with zero birefringence for magneto-optic waveguide devices," *J. Appl. Phys.*, **63**, 3099, (1988).

[22] K. Ando, N. Takeda, N. Koshizuka, and T. Okuda, "Annealing effect on growth-induced optical birefringence in liquid-phase-epitaxy-grown Bi-substituted iron garnet films," *J. Appl. Phys.*, **57**, 1277, (1984).

[23] R. Wolfe, R. A. Lieberman, V. J. Fratello, R. E. Scotti, and N. Kopylov, "Etch-tuned ridged waveguide magneto-optic isolator," *Appl. Phys. Lett.*, **56**, 426, (1990).

[24] R. Wolfe, V. J. Fratello, and M. McGlashan-Powell, "Elimination of birefringence in garnet films for magneto-optic waveguide devices," *Appl. Phys. Letts.*, **51**, 1221, (1987).

[25] R. Wolfe, J. Hegarty, J. F. Dillon, Jr., L. C. Luther, G. K. Celler, L. E. Trimble, and C. S. Dorsey, ''Thin-film waveguide magneto-optic isolator,'' *Appl. Phys. Lett.* **46**, 817 (1985).

[26] P.K. Tien and R.J. Martin, R. Wolfe, R.C. Le Craw, and S.L. Blank, "Switching and modulation of light in magneto-optic waveguides of garnet films," *Appl. Phys. Lett.* **21**, 394 (1972).

[27]B. M. Holmesa and D. C. Hutchings, "Demonstration of quasi-phase-matched nonreciprocal polarization rotation in III-V semiconductor waveguides incorporating magneto-optic upper claddings," *Appl. Phys. Lett.* **88**, 061116 (2006).

[28] H. Dammann, E. Pross, G. Rabe, and W. Tolksdorf, ''45° waveguide isolators with phase mismatch,'' *Appl. Phys. Lett.* **56**, 1302, (1990).

[29] R. Wolfe, J. F. Dillon, Jr., R. A. Liebermann, and V. J. Fratello, ''Broadband magneto-optic waveguide isolator,'' *Appl. Phys. Lett.* **57**, 960,(1990).

[30] F. Auracher and H. H. White, "A new design for an integrated optical isolator," *Opt. Commun.*, **13**, pp. 435, (1975).

[31] N. Bahlmann, M. Lohmeyer, M. Wallenhorst, H. Dötsch, and P. Hertel, ''A comparison of an improved design for two integrated optical isolators based on nonreciprocal Mach–Zehnder interferometry,'' in *Symposium Proceedings on High Density Magnetic Recording and Integrated Magnetooptics: Materials and Devices*, **517**, 513, (1998).

[32] T. Mizumoto, S. Mashimo, T. Ida, and Y. Naito, "In-Plane Magnetized Rare Earth Iron Garnet for a Waveguide Optical Isolator Employing Nonreciprocal Phase Shift," *IEEE Trans. Magn.* **29**, 3417, (1993).

[33] J. Fujita, M. Levy, R. U. Ahmad, R. M. Osgood Jr., M. Randles, C. Gutierrez, and R. Villareal, "Observation of optical isolation based on nonreciprocal phase shift in a Mach–Zehnder interferometer," *Appl. Phys. Lett.*, **75**, 998, (1999).

[34] J. Fujita, M. Levy, R.M. Osgood Jr., L.Wilkens, and H. Dötsch, "Waveguide optical isolator based on Mach-Zehnder interferometer," *Appl. Phys. Lett.*, 76,. 2158, (2000).

[35] M. Wallenhorst, M. Niemöller, H. Dötsch, P. Hertel, R. Gerhardt, and B. Gather, "Enhancement of the nonreciprocal magneto-optic effect of TM modes using iron garnet double layers with opposite Faraday rotation," *J. Appl. Phys.*, **77**, 2902, (1995).

[36] N. Bahlmann, V. Chandrasekhara, A. Erdmann, R. Gerhardt, P. Hertel, R. Lehmann, D. Salz, F. Schroteler, M. Wallenhorst, and H. Dotsch, " Improved design of magnetooptic rib waveguides for optical isolators," *J. Lightwave Technol.*, **16,** 818, (1998).

[37] H. Yokoi, Y. Shoji, E. Shin, and T. Mizumoto, "Interferometric optical isolator employing a nonreciprocal phase shift operated in a unidirectional magnetic field," *Appl. Opt.*, **43**, 4745, (2004).

[38] A. F. Popkov, M. Fehndrich, M. Lohmeyer, and H. Dötsch, ''Nonreciprocal TE mode phase shift by domain walls in magneto-optic rib waveguides,'' *Appl. Phys. Lett.* **72**, 2508, (1998).

[39] M. Fehndrich, A. Josef, L. Wilkens, J. Kleine-Börger, N. Bahlmann, M. Lohmeyer, P. Hertel, and H. Dötsch, ''Experimental investigation of the nonreciprocal phase shift of a transverse electric mode in a magneto-optic rib waveguide,'' *Appl. Phys. Lett.,* **74**, 2918, (1999).

[40] N. Bahlmann, M. Lohmeyer, H. Dötsch, and P. Hertel, ''Finite-element analysis of nonreciprocal phase shift for TE modes in magnetooptic rib waveguides with a compensation wall,'' *IEEE J. Quantum Electron.* **35**, 250, (1999).

[41] L. Wilkens, D. Tra¨ger, A. F. Popkov, A. Alexeev, and H. Dötsch, ''Nonreciprocal phase shift of TE modes induced by a compensation wall in a magneto-optic rib waveguide,'' *Appl. Phys. Lett.,* **79**, 4292, (2001).

[42] N. Bahlmann, M. Lohmeyer, H. Dötsch, and P. Hertel, ''Integrated magneto-optic Mach–Zehnder isolator for TE modes,'' *Electron. Lett.*, **34**, 2122, (1998).

[43] O. Zhuromskyy, M. Lohmeyer, N. Bahlmann, H. Dötsch, P. Hertel, and A. F. Popkov, ''Analysis of polarization independent Mach–Zehnder-type integrated optical isolator,'' *J. Lightwave Technol.,* **17**, 1200, (1999).

[44] J. Fujita, M. Levy, R. M. Osgood, Jr., L. Wilkens, and H. Dötsch, ''Polarization-independent waveguide optical isolator based on nonreciprocal phase shift,'' *IEEE Photonics Technol. Lett.* **12**, 1510, (2000).

[45] O. Zhuromskyy, H. Dötsch, M. Lohmeyer, L. Wilkens, and P. Hertel, ''Magneto-optical waveguides with polarizationindependent nonreciprocal phase shift,'' *J. Lightwave Technol.* **19**, 214, (2001).

[46] J. Z. Huang, R. Scarmozzino, G. Nagy, M. J. Steel, and R. M. Osgood, Jr., "Realization of a Compact and Single-Mode Optical Passive Polarization Converter", *IEEE Photon. Techno. lett.*, **12**, 317, (2000).

[47] D. C. Hutchings, "Prospects for the implementation of magneto-optic elements in optoelectronic integrated circuits: a personal perspective," *J. Phys. D: Appl. Phys.* **36**, 2222, (2003).

[48] K. Sakurai, H. Yokoi, T. Mizumoto, D. Miyashita and Y. Nakano, "Fabrication of Semiconductor Laser for Integration with Optical Isolator," *Jpn. J. Appl. Phys.* **43**, 1388, (2004).

[49] H. Yokoi, T. Mizumoto, "Proposed configuration of integrated optical isolator employing wafer-direct bonding technique," *Electro. Lett.*, **33**, 1787, (1997).

[50] H. Yokoi, T. Mizumoto, N. Shinjo, N. Futakuchi, and Y. Nakano, "Demonstration of an Optical Isolator with a Semiconductor Guiding Layer that was Obtained by Use of a Nonreciprocal Phase Shift," *Appl. Opt.* **39**, 6158, (2000).

[51] R. L. Espinola, T. Izuhara, M. -C. Tsai, R. M. Osgood, Jr., and H. Dötsch, "Magneto-optical nonreciprocal phase shift in garnet/silicon-on-insulator waveguides," *Opt. Lett.* **29**, 941, (2004)

[52] H. Yokoi, Y. Shoji, T. Mizumoto, "Calculation of nonreciprocal phase shift in magnetooptic waveguide with Si guiding layer," *Jpn. J. Appl. Phys.* **43**, 5871, (2004).

[53] H. Yokio, "Proposed Configuration of Optical Isolator with $TiO_2$/Magnetic Garnet Waveguide", *Jpn. J. Appl. Phys.* **44**, 3992, (2005).

[54] T.Mizumoto, "(Invited) Waveguide optical isolator integratable to LDs and SOAs," Optical Fiber Communication Conference 2004 (OFC2004), Los Angeles, TuE5 (Feb., 2004).

[55] M. Bouda and Y. Nakano, "Development of metal-organic vapor phase diffusion enhanced selective area epitaxy, a novel metal-organic vapor phase epitaxy selective area growth technique, and its application to multi-mode interference device fabrication," *Jpn. J. Appl. Phys.*, **38**, 1029, (1999).

[56] H. Yokoi, T. Mizumoto, K. Maru and Y. Naito, "Direct bonding between InP and rare earth iron garnet grown on $Gd_3Ga_5O_{12}$ substrate by liquid phase epitaxy," *Electron. Lett.*, **31**, 1612, (1995).

[57] H. Yokoi, T. Mizumoto, K. Maru and Y. Naito, "Improved Heat Treatment for Wafer Direct Bonding between Semiconductors and Magnetic Garnets," *Jpn. J. Appl. Phys.* **36**, 2784, (1997).

[58] H. Yokoi, T. Mizumoto and Y. Shoji, "Optical nonreciprocal devices with a silicon guiding layer fabricated by wafer bonding," *Appl. Opt.*, **42**, 6605, (2003).

[59] T. Izuhara, M. Levy, and R. M. Osgood, Jr., "Direct wafer bonding and transfer of 10-μm-thick magnetic garnet films onto semiconductor surfaces," *Appl. Phys. Lett.*, **76**, 1261, (2000).

[60] F. Rachford, M. Levy, R. M. Osgood Jr., A. Kumar, and H. Bakhru, "Magnetization and FMR studies in implanted and crystal ion sliced Bi-YIG films," *J. Appl. Phys.*, **85**, 5217, (1999).

[61] M. Levy, R. M. Osgood Jr., A. Kumar, and H. Bakhru, "Crystal ionslicing in single-crystal magnetic garnet films," *J. Appl. Phys.*, **83**, 6759, (1998).

[62] H. Yokoi, T. Waniishi, T. Mizumoto, M. Shimizu, "Integration of terraced laser diode and garnet crystals by wafer direct bonding," *Jpn. J. Appl. Phys.*, **40**, 3463, (2001).

[63] B.J.H. Stadler and A. Gopinath, "Magneto-optical garnet films made by reactive sputtering," *IEEE Trans. Magn.* **36**, 3957, (2000).

[64] S-Y. Sung, X-Y. Qi, S. K. Mondal, and B.J.H. Stadler, "Partial pressure differential and rapid thermal annealing for integrated yttrium iron garnet (YIG)," *Mat. Res. Soc. Symp. Proc.*,**817**, L8.3.1, (2004).

[65] S-Y. Sung, X-Y. Qi, and B.J.H. Stadler, "Integrating yttrium iron garnet onto nongarnet substrates with faster deposition rates and high reliability," *Appl. Phys. Lett.*, **87**, 121111, (2005).

[66] L. J. C. Rivera, S-Y. Sung, J. Cassada, M. R. M. Cruz, and B.J.H. Stadler, "Materials issues in the layers required for integrated magneto-optical isolators," *Mat. Res. Soc. Symp. Proc.*,**722**, K9.15.1, (2002).

[67] B.J.H. Stadler, K. Vaccaro, P. Yip, Jo. Lorenzo, Y-Q. Li, and M. Cherif, "Integration of magneto-optical garnet films by metal-organic chemical vapor deposition," *IEEE Trans. Magn.* **38**, 1564, (2002).

[68] A. K. Bandyopadhyay, S.E. Rios, S. Fritz, J. Garcia, J. Contreras, and C. J. Gutierrez, "Ion beam sputter-fabrication of Bi-YIG films for magnetic photonic applications," *IEEE Trans. Magn.* **40**, 2805, (2004).

[69] B.M. david, C. Hutchings and J. J. Bregenzer, "Experiments towards the realization of a monolithically-integrated optical isolator incorporating quasi-phase matched magneto-optical effects," *Mat. Res. Soc. Symp. Proc.*,**834**, J4.4.1, (2005).

[70] B. J.H. Stadler, Y. Li, M. Cherif, K. Vaccaro and J. Lorenzo, "Doped yttrium iron garnet (YIG) thin films for integrated magneto-optical applications," in *MRS Proc.* **442**, 389, (1996).

[71] A. Rajamani, G. F. Dionne, D. Bono, and C. A. Ross, "Faraday rotation, ferromagnetism, and optical properties in Fe-doped $BaTiO_3$," *J. Appl. Phys.*, **98**, 063907, (2005).

[72] H. Akinaga, S. Miyanishi, K. Tanaka, W. Van Roy, and K. Onodera, "Magneto-optical properties and the potential application of GaAs with magnetic MnAs nanoclusters," *Appl. Phys. Lett.* **76**, 97, (2000).

[73] H. shimizu and M. Tanaka, "Magneto-optical properties of semiconductor-based superlattices having GaAs with MnAs nanoclusters," *J. Appl. Phys.*, **89**, 7281, (2001).

[74] T. R. Zaman, X. Guo, and R. J. Ram, "Faraday rotation in an InP waveguide," *Appl. Phys. Lett.*, **90**, 023514, (2007).

[75] W. Zayets and K. Ando, "Magneto-optical mode conversion in $Cd_{1-x}Mn_xTe$ waveguide on GaAs substrate," *Appl. Phys. Lett.*, **77**, 1593, (2000).

[76] V. Zayets, M. C. Debnath, and K. Ando, "Complete magneto-optical waveguide mode conversion in $Cd_{1-x}Mn_xTe$ waveguide on GaAs substrate," *Appl. Phys. Letts.*, **84**, 565, (2004).

[77] M. Takenaka and Y. Nakano, "Proposal of a novel semiconductor optical waveguide isolator," presented at the 11$^{th}$ International Conference on Indium Phosphide and Related Materials, Davos, Switzerland, May 16-20, (1999).

[78] W.Zaets and K. Ando, "Optical waveguide isolator based on nonreciprocal loss/gain amplifier covered by ferromagnetic layer," *IEEE Photon Technol. Lett.* **11**, 1012, (1999).

[79] K. Postava, M. Vanwollegham, D. Van Thourhout, R. Baets, Š. Višňovský, P. Beauvillain, J. Pištora, "Modeling of a novel InP-based monolithically integrated magneto-optical waveguide isolator," *J. Opt. Soc. Am. B* **22**, 261, (2005).

[80] M. Vanwolleghem, W. Van Parys, D. Van Thourhout, R. Baets, F. Lelarge, O. Gauthier-Lafaye, B. Thedrez, R. Wirix-Speetjens, and L. Lagae, "Experimental demonstration of nonreciprocal amplified spontaneous emission in a CoFe clad semiconductor optical amplifier for use as an integrated optical isolator," *Appl. Phys. Lett.*, **85,** 3980 (2004).

[81] W. Van. Parys, B. Moeyersoon, D. Van. Thourhout, R. Baets, M. Vanwolleghem, B. Dagens, J. Decobert, O. L. Gouezigou, D. Make, R. Vanheertum and L. Lagae, "Transverse magnetic mode nonreciprocal propagation in an amplifying AlGaInAs/InP optical waveguide isolator," *Appl. Phys. Lett.*, **88**, 071115 (2006).

[82] T. Amemiya, Y. Nakano, H. Shimizu, M. Yokoyama, P. N. Hai, and M. Tanaka, "1.54-μm, TM-mode waveguide optical isolator based on nonreciprocal-loss phenomenon; device design to reduce insertion loss," To be published in OSA, 2007.

[83] H. Shimizu and Y. Nakano, "First demonstration of TE mode nonreciprocal propagation in an InGaAsP/InP active waveguide for an integratable optical isolator," *Jpn. J. Appl. Phys*, **43** L1561, (2004).

[84] H. Shimizu and Y. Nakano, "Fabrication and characterization of an InGaAsP/InP active waveguide optical isolator with 14.7 dB/mm TE mode nonreciprocal attenuation," *J. Lightwave. Technol.*, **24**, 38, (2006).

[85] United States Patent 7113676, "Planar waveguide optical isolator in thin silicon-on-isolator (SOI) structure," (2006).

[86] S. Bhandare, S. K. Ibrahim, d. Sandel, H. Zhang, F. Wüst, and R. Noé, "Novel nonmagnetic 30-dB traveling-wave single-sideband optical isolator integrated in III/V material," *IEEE J. Selected Topics in Quantum Electronics*, **11**, 417, (2005).

[87] Eblanaphotonics http://www.eblanaphotonics.com

[88] United States Patent 6891870, "Distributed feedback laser for isolator-free operation," (2005).

[89] Oki Electric Industry Co., Ltd. http://www.oki.com

[90] Electronicast and customer data.